

Microanalysis of carbonate cement $\delta^{18}\text{O}$ in a CO_2 -storage system seal: Insights into the diagenetic history of the Eau Claire Formation (Upper Cambrian), Illinois Basin

Maciej G. Śliwiński, Reinhard Kozdon, Kouki Kitajima, Adam Denny, and John W. Valley

AAPG Bulletin, v. 100, no. 6 (June 2016), pp. 1003–1031

Copyright ©2016. The American Association of Petroleum Geologists. All rights reserved.

APPENDIX 1: ANALYTICAL METHODS

Sample Preparation

Samples for in situ $\delta^{18}\text{O}$ analysis were cast into 25-mm-diameter epoxy mounts (Buehler EpoxyCure), taking care to position areas of interest within a 5-mm radius of the geometric center; this was done to minimize any potential fractionation effects associated with a sample's position relative to the focusing axis within the analysis chamber (Kita et al., 2009; Valley and Kita, 2009). Several grains of a running standard (end-member dolomite UW6220, $\delta^{18}\text{O} = 22.60\text{‰}$ Vienna standard mean ocean water [VSMOW], -8.1‰ Vienna Peedee belemnite [VPDB]; Śliwiński et al., 2015) were embedded in the center of each mount, which was then polished to a 0.25- μm finish using oil-based polycrystalline diamond suspensions (Buehler MetaDi Supreme) and Allied TECH-Cloth pads. Care was taken to keep polishing relief between mineral phases of contrasting hardness (e.g., carbonate cements in quartz-rich sandstones) to less than a few micrometers. Prior to analysis, sample mounts were cleaned with deionized water and ethanol and coated with carbon (25-nm thickness) to make sample surfaces electrically conductive.

Oxygen Isotope Analyses by Secondary Ion Mass Spectrometry

In situ $\delta^{18}\text{O}$ measurements were performed using a CAMECA IMS 1280 large-radius multicollector ion microprobe at the Wisconsin Secondary Ion Mass Spectrometer (WiscSIMS) Laboratory (Department of Geoscience, University of Wisconsin–Madison). The sample data presented here were collected during four analytical sessions throughout the course

of 1 yr: two 10- μm -diameter spot-size sessions (session S1, September 23–25, 2013, and session S7, May 13–16, 2014) and two 3- μm spot-size sessions (session S4, February 24–27, 2014, and session S8, May 22–25, 2014). The full data set is provided in Appendices 4 and 5. The analytical conditions employed were the same as those described in Śliwiński et al. (2015).

The analytical accuracy of oxygen–isotope ratio measurements by secondary ion mass spectrometry (SIMS) is affected by instrumental mass fractionation (referred to here as “SIMS $\delta^{18}\text{O}$ bias”; Hervig et al., 1992; Kita et al., 2009; Valley and Kita, 2009), a component of which is systematically related to the chemical composition and crystal structure of a sample. A calibration scheme for correcting SIMS $\delta^{18}\text{O}$ bias for carbonate mineral compositions along the dolomite–ankerite solid solution series was reported by Śliwiński et al. (2015) and employed here for reducing sample data. The calibration relates the magnitude of SIMS $\delta^{18}\text{O}$ bias to the Fe number [$=\text{Fe}/(\text{Mg} + \text{Fe})$ molar ratio] of dolomite–ankerite using the three-parameter Hill equation (e.g., review of Goutelle et al., 2008), which elegantly describes empirical relationships of the “component concentration” versus “measured effect” type in systems that behave nonlinearly and reach saturation; it is characterized by two curve-shape parameters (n and k) and an analytical session-specific calibration scaling factor ($\text{bias}^*_{\text{max}}$). Although it is common in SIMS analyses for the magnitude of instrumental $\delta^{18}\text{O}$ bias to vary from session to session, the overall distribution of calibration standard data points in relation to one another remains remarkably consistent, with the values of both Hill shape parameters (n and k) remaining invariant for the IMS 1280 instrument and tuning protocols at the WiscSIMS lab. Thus, it is best in every analysis session to analyze a

series of standards between dolomite and ankerite to construct a working curve, but even if only two standards from the dolomite–ankerite solid solution series are measured (end-member dolomite in addition to one ankerite from the opposite end of the series), a calibration curve can still be established, albeit with a slight increase in the analytical uncertainty (by an additional $\sim 0.3\%$). The analytical precision is typically $\pm 0.3\%$ (two standard deviations [2SD]) for 10- μm -diameter sample spot analyses and $\pm 0.7\%$ (2SD) for 3- μm spots, based on the spot-to-spot reproducibility (number of analysis [n] = 8) of a running standard (end-member dolomite, UW6220) that “brackets” each set of 10 sample analyses. The accuracy of sample analyses is, in part, determined by the calibration residual, which is a measure of how well the SIMS $\delta^{18}\text{O}$ bias correction scheme reproduces standard data in relation to the certified reference material (RM) NBS-19; for 10- μm spot-size sessions, the residual is constrained to 0.3% for a suite of 13 dolomite–ankerite standards, whereas it is within 0.4% when performing analyses using a 3- μm spot (Śliwiński et al., 2015).

Measured isotope ratios are reported using the conventional δ notation expressed in per mil relative to the VSMOW and VPDB $\delta^{18}\text{O}$ scales.

Chemical Analysis (by Electron Probe Microanalysis)

To correct each in situ carbonate $\delta^{18}\text{O}$ analysis for SIMS instrumental bias, it is necessary to have knowledge of the cation composition of the sample material sputtered from each sample pit. Chemical analyses in the immediate vicinity of each SIMS pit (detailed below) were performed by electron probe microanalysis (EPMA) using a CAMECA SX-51 at the Cameron Electron Microprobe Laboratory (Department of Geoscience, University of Wisconsin–Madison).

The electron microprobe was operated at 15 keV and 10 nA; care was taken to minimize beam damage to carbonate samples by performing analyses with the electron beam preferentially defocused to a 5- μm diameter where possible. However, the narrow thickness of certain compositional zones at times necessitated the use of a 2- μm -diameter beam. Monte Carlo simulations using Casino software (v2.41; Drouin et al., 2007) indicate that under these

conditions, a 2- μm -diameter beam produces an interaction volume in dolomite and ankerite with a surface footprint approximately 3–4 μm in diameter. Thus, to avoid any potential edge effects, EPMA analyses were performed at least 5 μm away from 3- μm SIMS pits (using a 2- μm electron beam) and approximately 10 μm away from 10- μm SIMS pits (using a 5- μm electron beam). Characteristic x-ray intensities were measured for 10 s on each spectral peak and on two background positions (one on either side of each peak). During the course of a point analysis, the intensities of characteristic x-rays fluorescing from electron beam-sensitive materials can drift; this is corrected by a feature in Probe for EPMA software (Donovan et al., 2007) called TDI (time-dependent intensity), where data plotted in “measured x-ray intensity” versus “time” space are first detrended before the application of ZAF corrections (i.e., corrections for sample matrix effects, based on mean atomic number [Z], x-ray absorption [A], and x-ray fluorescence [F]).

The electron microprobe was standardized with the following RMs: Delight Dolomite (RM for Ca, analyzed using a pentaerythritol [PET] crystal, and RM for Mg, using a thallium acid phthalate [TAP] crystal), Callender Calcite (alternate RM for Ca), USNM 460 Siderite (RM for Fe, using a lithium fluoride [LiF] crystal), rhodochrosite (RM for Mn, using a LiF crystal), and strontianite (RM for Sr, using a TAP crystal). Data were collected during five analytical sessions throughout the course of a year (Fall 2013–Summer 2014). Based on replicate measurements ($n = 5$ –10) of the above RMs during each session, the elemental concentrations determined for each of the cations are precise to within 2.5% relative (relative standard deviation), whereas deviations from accepted values are constrained to within 5% relative.

Sample Imaging by Scanning Electron Microscope

Extensive characterization of carbonate cements in sandstone samples by backscattered electron (BSE) and cathodoluminescence (CL) imaging (using a Hitachi S3400-N scanning electron microscope [SEM]) was employed to identify areas of interest prior to in situ $\delta^{18}\text{O}$ analyses by SIMS and then again after SIMS analysis to verify that sample pits were

indeed placed where intended. High-resolution secondary electron images were acquired prior to SIMS analysis to identify characteristic features on sample surfaces (e.g., cracks, cavities, etc.) to aid in navigating and to allow for triangulating target positions in the reflected light optics of the SIMS sample viewer; secondary electron imaging was used again after analysis to assess the overall quality of each sputtered SIMS pit by revealing its surface texture. Data points were flagged and excluded if pits were found to partially overlap epoxy or showed any of the following features: cracks, epoxy, cavities (larger than ~1–2 μm), inclusions of other minerals, or any “shelves” or “ledges” that detract from an otherwise regular appearance of the pit sputtered by the ion beam. Cathodoluminescence imaging was employed to identify and to image the earliest formed, commonly luminescent generations of carbonate cement. Following the method of Reed and Milliken (2003), a broadband, short-wavelength (ultraviolet-blue range) filter was employed to avoid streaking in SEM-CL images that results from carbonate phosphorescence.

Bulk Mineralogy and Clay Speciation Analyses by X-Ray Diffraction

Five Eau Claire Formation shale samples from different burial depths across the Illinois Basin were submitted to ActLabs (Ancaster, Ontario, Canada) for clay mineral analysis by x-ray diffraction. A part of each powdered sample was mixed with 10 wt. % corundum powder and loaded into a standard back-fill holder. Corundum was used as an internal standard to determine the x-ray amorphous content of the samples. The abundances of the crystalline mineral phases were determined using the Rietveld refinement method, which is based on reproducing an observed diffraction pattern through modeling with crystallographic parameters. A part of each sample was dispersed in distilled water and clay minerals in the less than 2- μm fraction separated by gravity settling of particles in suspension. Oriented slides of the less than 2- μm fraction were prepared by placing a part of the suspension onto a glass slide. To identify expandable clay minerals, the oriented slides were analyzed after (1) air drying, (2) saturation with ethylene glycol, and (3) subsequent heating at 375°C (~710°F) for 1 hr. The semiquantitative

amounts of the different clay minerals in the less than 2- μm fraction were determined based on calculations of basal-peak areas.

The x-ray diffraction analysis was performed on a Panalytical X'Pert Pro diffractometer equipped with a Cu x-ray source and an X'Celerator detector. The operating conditions were as follows: 40 kV and 40 mA, range 4°–70° 2θ for random powder mounts and 3°–35° 2θ for oriented clay mineral preparations, step size 0.017° 2θ , time per step 50.165 s, fixed divergence slit (1/4°), and sample rotation 1 rev/s.

The abundances of illite and smectite in clay mineral separates can be assessed using Środoń's (1984) intensity ratio (IR). This parameter compares x-ray IRs of the illite 001 and 003 diffraction peaks measured in oriented clay mounts before and after glycolation and is very sensitive to the presence of swelling (smectite) layers ($\text{IR} = [\text{001}/\text{003}]_{\text{air dried}} / [\text{001}/\text{003}]_{\text{glycolated}}$). Swelling has occurred if $\text{IR} > 1.0$; values less than approximately 1.5 are generally consistent with less than 15% smectite (Środoń, 1984).

REFERENCES CITED

- Donovan, J. J., D. Kremser, and J. H. Fournelle, 2007, Probe For Windows user's guide and reference, enterprise edition: Eugene, Oregon, Probe Software, 355 p.
- Drouin, D., A. Réal Couture, D. Joly, X. Tastet, V. Aimez, and G. Gauvin, 2007, CASION V2.42—A fast and easy-to-use modeling tool for scanning electron microscopy and microanalysis users: Scanning, v. 29, p. 92–101, doi:10.1002/sca.20000.
- Goutelle, S., M. Maurin, F. Rougier, X. Barbaut, L. Bourguignon, M. Ducher, and P. Maire, 2008, The Hill equation: A review of its capabilities in pharmacological modelling: Fundamental and Clinical Pharmacology, v. 22, p. 633–648, doi:10.1111/j.1472-8206.2008.00633.x.
- Hervig, R. L., P. Williams, R. M. Thomas, S. N. Schauer, and I. M. Steele, 1992, Microanalysis of oxygen isotopes in insulators by secondary ion mass spectrometry: International Journal of Mass Spectrometry and Ion Processes, v. 120, p. 45–63, doi:10.1016/0168-1176(92)80051-2.
- Kita, N. T., T. Ushikubo, B. Fu, and J. W. Valley, 2009, High precision SIMS oxygen isotope analysis and the effect of sample topography: Chemical Geology, v. 264, p. 43–57, doi:10.1016/j.chemgeo.2009.02.012.
- Reed, R. M., and K. L. Milliken, 2003, How to overcome imaging problems associated with carbonate minerals on SEM-based cathodoluminescence systems: Journal of Sedimentary Research, v. 73, no. 2, p. 328–332, doi:10.1306/081002730328.
- Śliwiński, M. G., K. Kitajima, R. Kozdon, M. J. Spicuzza, J. H. Fournelle, A. Denny, and J. W. Valley, 2015, Secondary ion mass spectrometry bias on isotope ratios

in dolomite–ankerite, part I: $d^{18}\text{O}$ matrix effects: Geostandards and Geoanalytical Research, doi:10.1111/j.1751-908X.2015.00364.x.

- Šrodon, J., 1984, X-ray powder diffraction identification of illitic materials: *Clays and Clay Minerals*, v. 32, no. 5, p. 337–349.
- Valley, J. W., and N. T. Kita, 2009, In situ oxygen isotope geochemistry by ion microprobe, in M. Fayek, ed., Secondary ion mass spectrometry in the earth sciences: Québec, Québec, Canada, Mineralogical Association of Canada Short Course 41, p. 19–63.

APPENDIX 2: ABBREVIATED CORE DESCRIPTIONS

Eau Claire Formation Interval, Illinois Basin

The purpose of the following is to provide a lithostratigraphic context to the samples that were collected and analyzed for this study. Sandstone beds within the predominantly silty–shaly Eau Claire Formation were sampled at three cored localities (refer to Figure 1 and Table 1 in main text) representing different sediment burial depths: (1) on the Wisconsin arch (sample SS-1, maximum burial depth <0.5 km (~1500 ft); see discussion in the Significance of Paleodepth-Related Differences in Carbonate Cement $\Delta^{18}\text{O}$ [Early–Late] section), (2) on the basin margin in northern Illinois (SS-2, maximum burial depth ~1 km [3500 ft]), and (3) in the central Illinois Basin (SS-3, maximum burial depth ~2 km [6500 ft]).

Historical coring to the basal Mt. Simon Sandstone of the Illinois Basin often did not aim for a recovery of the overlying Eau Claire Formation interval (R. Mumm, 2013, personal communication). Thus, only a relatively small number of cores exist with the Eau Claire Formation intact or present altogether, hindering a thorough characterization of the stratigraphy and limiting the wherewithal to laterally correlate specific lithofacies across the basin (Neufelder et al., 2012).

Legacy porosity and permeability data are provided where available.

Core C131467 (Dane County, Wisconsin; API Number: Not Applicable)

Depth of sandstone bed sampled for this study: 277.9 ft (84.7 m) (sample SS-1).

Aswasereelert et al. (2008) divided the Eau Claire Formation of west to southcentral Wisconsin into five distinct lithofacies (A–E; see table 1 therein) that

represent different paleowater depths and depositional environments (outer shelf to shore face) of an epeiric shelf. Only the finer-grained, outer shelf facies (A and B) are present at this cored locality; an overview of the lithostratigraphy is shown in Figure A.1 (see figure 13 in Aswasereelert et al., 2008 for a more comprehensive description).

- Lithofacies A: This facies consists of mudstone and siltstone with minor, very thin-bedded (0.1–1 cm [\sim 0.0625–0.375 in.]) sandstone beds. This designation was given to cored intervals comprised of at least one 1-ft (\sim 30-cm) interval of very thin- (0.1–1 cm [\sim 0.0625–0.375 in.]) to thin-bedded (1–10 cm) mudstone and/or siltstone.
- Lithofacies B: This facies consists of thin-bedded sandstone beds (1–10 cm [\sim 0.375–4 in.], generally <5 cm [\sim 2 in.]) with very thin siltstone and mudstone interbeds (0.1–1 cm [\sim 0.0625–0.375 in.]).
- In southern Wisconsin, the Eau Claire Formation is an important regional aquitard (Aswasereelert, 2005; Aswasereelert et al., 2008).

Core C12996 (UPH-3) (Stephenson County, Illinois; API Number: 121772131700)

Depth of sandstone bed sampled for this study: 1217.3 ft (371 m) (sample SS-2).

The following lithostratigraphic overview pertains to core UPH-1 (API number: 121772131500), drilled approximately 4.5 mi (\sim 7 km) north of the core sampled for this study (C12996/UPH-3). The depth of the sandstone bed sampled in core C12996/UPH-3 (1217.3 ft [371 m]) was correlated to within several feet with the depth of the equivalent bed in core UPH-1 (position indicated in Table A.1 at 1101 ft [335.6 m]) based on the following reference horizons: (1) the depth of the contact between the Mt. Simon and the Eau Claire Formations (UPH-1: 1165 ft [355.1 m]; UPH-3: 1308 ft [398.7 m]) and (2) the depth of unique carbonate beds (UPH-1: \sim 1046.7–1047 (319–319.1 m) and 1050.5–1051.5 ft [320.2–320.5 m]; UPH-3: \sim 1191.6 ft [363.2 m]).

Core C4006 (Champaign County, Illinois; API Number: 120190012800)

Depth of sandstone bed sampled for this study: 3857 ft (1175.6 m) (sample SS-3).

The sources of the following information are core descriptions from a well folder, provided by the Geological Records Unit of the Illinois State Geological Survey.

The Eau Claire Formation interval (3305–3993 ft [1007–1217.1 m]) was cored from 3751–3992 ft (1143.3–1216.8 m). The core is no longer complete; it has been reduced to “chips” that represent approximately 15% of the original core material. Table A.2 below provides a summarized overview of the lithologies present and the range of porosity and permeability values for the different depth intervals (measurements performed by Core Laboratories, Inc., Oklahoma City, Oklahoma, 1959). The position of the sandstone bed sampled for this study (sample SS-3, 3857 ft [1175.6 m]) is indicated.

REFERENCES CITED

- Aswasereelert, W., 2005, Facies distribution and stacking of the Eau Claire Formation, Wisconsin: Implications of thin shale-rich strata in fluid flow, Master's thesis, University of Wisconsin–Madison, Madison, Wisconsin, 200 p.
- Aswasereelert, W., J. A. Simo, and D. L. LePain, 2008, Deposition of the Cambrian Eau Claire Formation, Wisconsin: Hydrostratigraphic implications of fine-grained cratonic sandstones: *Geoscience Wisconsin*, v. 19, no. 1, p. 1–21.
- Neufelder, R. J., B. B. Bowen, R. W. Lahann, and J. A. Rupp, 2012, Lithologic, mineralogical and petrophysical characteristics of the Eau Claire Formation: Complexities of a carbon storage system seal: *Environmental Geoscience*, v. 19, p. 81–104, doi:[10.1306/eg.02081211014](https://doi.org/10.1306/eg.02081211014).
- Śliwiński, M.G., K. Kitajima, R. Kozdon, M. J. Spicuzza, J. H. Fournelle, A. Denny, and J. W. Valley, 2015, Secondary ion mass spectrometry bias on isotope ratios in dolomite–ankerite, part I: $\delta^{18}\text{O}$ matrix effects: *Geostandards and Geoanalytical Research*, doi:[10.1111/j.1751-908X.2015.00364.x](https://doi.org/10.1111/j.1751-908X.2015.00364.x).
- Środoń, J., 1984, X-ray powder diffraction identification of illitic materials.: *Clays and Clay Minerals*, v. 32, no. 5, p. 337–349, doi:[10.1346/CCMN.1984.0320501](https://doi.org/10.1346/CCMN.1984.0320501).
- Valley, J. W., and N. T. Kita, 2009, In situ oxygen isotope geochemistry by ion microprobe, *in* M. Fayek, ed., *Secondary ion mass spectrometry in the earth sciences: Mineralogical Association of Canada Short Course 41*, p. 19–63.

Table A.1. Core UPH-1

Depth (ft [m])	Interval Thickness	Lithology
846–851 (257.9–259.4)	5 ft (1.5 m)	Sandstone with shale streaks
851–864 (259.4–263.3)	13 ft (4 m)	Shale
864–926 (263.3–282.2)	62 ft (18.9 m)	Interbedded siltstone–shale (centimeter scale)
926–927 (282.2–282.5)	1 ft (0.3 m)	Sandstone, heavily iron stained (thoroughly maroon)
927–930 (282.5–283.5)	3 ft (0.9 m)	Interbedded siltstone–shale (centimeter scale)
930–933 (283.5–284.4)	3 ft (0.9 m)	Sandstone, heavily iron stained (thoroughly maroon)
933–974 (284.4–296.9)	41 ft (12.5 m)	Clean sandstone
974–986 (296.9–300.5)	12 ft (3.7 m)	Shale and very shaly siltstone
986–993 (300.5–302.7)	7 ft (2.1 m)	Clean sandstone
993–1035 (302.7–315.5)	42 ft (12.8 m)	Sandstone with siltstone interbeds (centimeter–decimeter scale) and shale streaks
1035–1040 (315.5–317)	5 ft (1.5 m)	Clean sandstone
1040–1041 (317–317.3)	1 ft (0.3 m)	Carbonate (dolomite) bed
1041–1046 (317.3–318.8)	5 ft (1.5 m)	Sandstone, heavily dolomitized? (not clean in appearance)
1046.7–1047 (319.0–319.1)	0.3 ft (0.1 m)	Carbonate (dolomite) bed
1047–1048.5 (319.1–319.6)	1.5 ft (0.5 m)	Sandstone, heavily dolomitized? (not clean in appearance)
1048.5–1049.5 (319.6–319.9)	1 ft (0.3 m)	Carbonate (dolomite) bed; several inches of siltstone and/or shale near bottom
1049.5–1050.5 (319.9–320.2)	1 ft (0.3 m)	Sandstone, heavily dolomitized? (not clean in appearance)
1050.5–1051.5 (320.2–320.5)	1 ft (0.3 m)	Carbonate (dolomite) bed
1051.5–1054 (320.5–321.3)	2.5 ft (0.8 m)	Sandstone (not clean in appearance); some shale streaks
1054–1075 (321.3–327.7)	21 ft (6.4 m)	Mixed sandstone and siltstone with shale laminations
1075–1094 (327.7–333.5)	19 ft (5.8 m)	Mostly clean sandstone with some shale streaks and gray sandstone beds
1094–1107 (333.5–337.4)	13 ft (4 m)	Clean sandstone*
1107–1136 (337.4–346.3)	29 ft (8.8 m)	Mixed clean gray sandstone with some siltstone laminations and shale streaks
1136–1142 (346.3–348.1)	6 ft (1.8 m)	Interbedded sandstone, siltstone, and shale
1142–1165 (348.1–355.1)	23 ft (7 m)	Sandstone (not clean in appearance); some shale streaks

*Sandstone bed sampled at depth of 1217.3 ft (371 m) (sample SS-3) in core C12996/UPH-3, equivalent in this core (UPH-1) to a depth of approximately 1101 ft (335.6 m).

Table A.2. Core C4006

Interval Identification	Depth (ft [m])	Interval Thickness	Depth (ft [m])	Lithology	Porosity (%)	Kmax (mD)	K90 (mD)	Kvert (mD)
Core 4	3751-3801 (1143.3-1158.5)	50 ft (15.2 m)	-	Black shale	8.4-10.3	<0.1	-	<0.1
Core 5	3810-3823 (1161.3-1165.3)	13 ft (4 m)	-	Interbedded shale and siltstone	3.3-8.9	<0.1-16	<0.1-3.5	<0.1
Core 6	3823-3847 (1165.3-1172.6)	24 ft (7.3 m)	-	Missing	-	-	-	-
Core 7	3847-3870 (1172.6-1179.6)	23 ft (7 m)	-	Interbedded shale	3.5-8.9	<0.1-4.1	<0.1-3.8	<0.1-0.2
Core 7	3847-3870 (1172.6-1179.6)	23 ft (7 m)	3847-3856 (1172.6-1175.3)	Interbedded shale and siltstone in beds up to 3 in. thick (~50:50)	4.8-7.7	<0.1-0.1	<0.1	<0.1
Core 7	3847-3870 (1172.6-1179.6)	23 ft (7 m)	3856-3863 (1175.3-1177.4)	Interbedded sandstone and shale in beds 3-12 in. thick; shale represents approximately 20% of interval and is concentrated in beds 1-6 in. thick*	3.5-7.7	<0.1-4.1	<0.1-3.8	<0.1-0.2
Core 7	3847-3870 (1172.6-1179.6)	23 ft (7 m)	3863-3870 (1177.4-1179.6)	Silty sandstone with thin wavy shale streaks; 90% sandstone, 10% shale	5.5-8.9	<0.1-1.4	<0.1-1.2	<0.1-0.1
Core 8	3870-3940 (1179.6-1200.9)	49 ft (14.9 m)	-	Silty sandstone as above	5.6-10.3	<0.1-13	<0.1-13	<0.1-4.8
Core 8	3870-3940 (1179.6-1200.9)	49 ft (14.9 m)	3870-3880 (1179.6-1182.6)	Interbedded siltstone and sandstone; shaly zone in lower 2 ft	5.5-10.9	<0.1-3.7	<0.1-2.6	<0.1-3.6
Core 8	3870-3940 (1179.6-1200.9)	49 ft (14.9 m)	3880-3896 (1182.6-1187.5)	Mostly sandstone	5.5-10.2	<0.1-31	4.9-29	<0.1-10
Core 8	3870-3940 (1179.6-1200.9)	49 ft (14.9 m)	3896-3910 (1187.5-1191.8)	Interbedded siltstone and sandstone	5.8-7.6	<0.1-18	<0.1-17	<0.1-4.2
Core 8	3870-3940 (1179.6-1200.9)	49 ft (14.9 m)	3910-3925 (1191.8-1196.3)	Mostly sandstone	6.2-9.2	0.1-28	0.1-25	<0.1-5.5
Core 8	3870-3940 (1179.6-1200.9)	49 ft (14.9 m)	3925-3933 (1196.3-1198.8)	Interbedded siltstone and sandstone; numerous shale layers 0.125-0.5 in. thick	4.3-5.8	<0.1-2.5	<0.1-2.4	<0.1-2.5
Core 8	3870-3940 (1179.6-1200.9)	49 ft (14.9 m)	3933-3940 (1198.8-1200.9)	Mostly sandstone	7.4-10.7	1.0-2.9	0.9-2.2	<0.1-0.8

Abbreviations: Kmax = maximum permeability of core measured in the horizontal direction; Kvert = permeability of core measured in the vertical direction; K90 = permeability measured after 90° rotation from the direction of Kmax.
 *Sandstone bed sampled at depth of 3857 ft (1175.6 m) (sample SS-3).

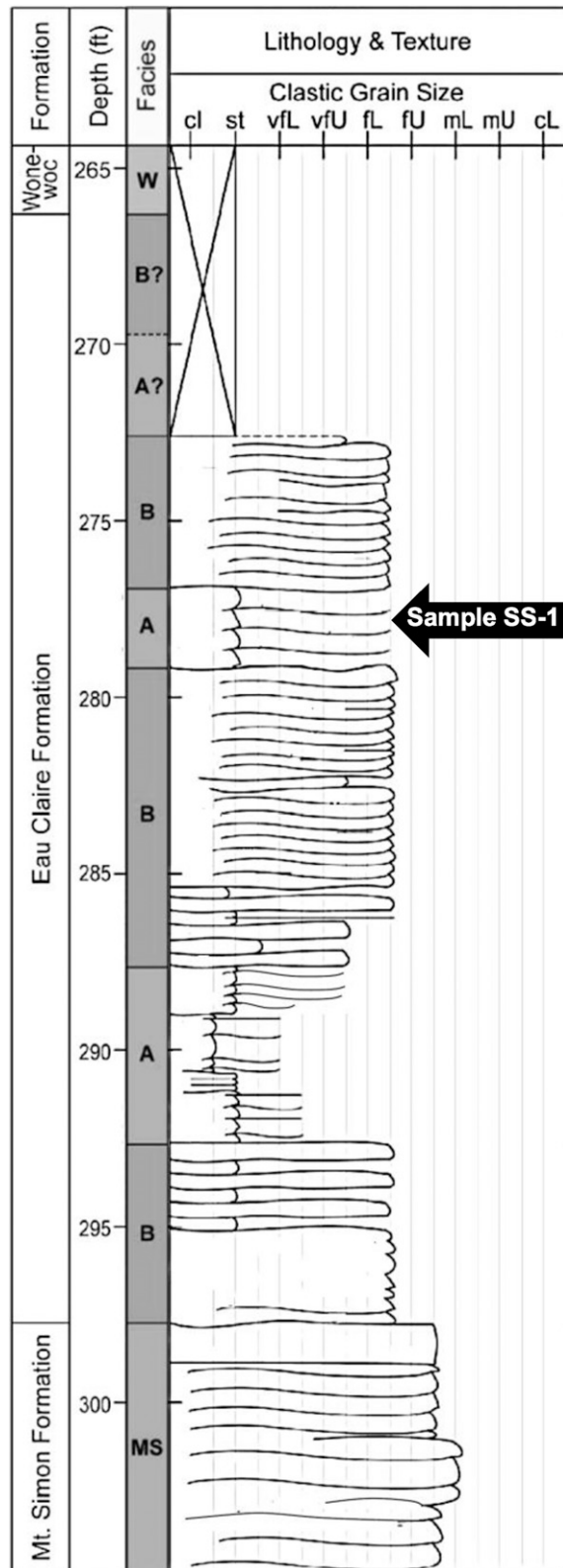
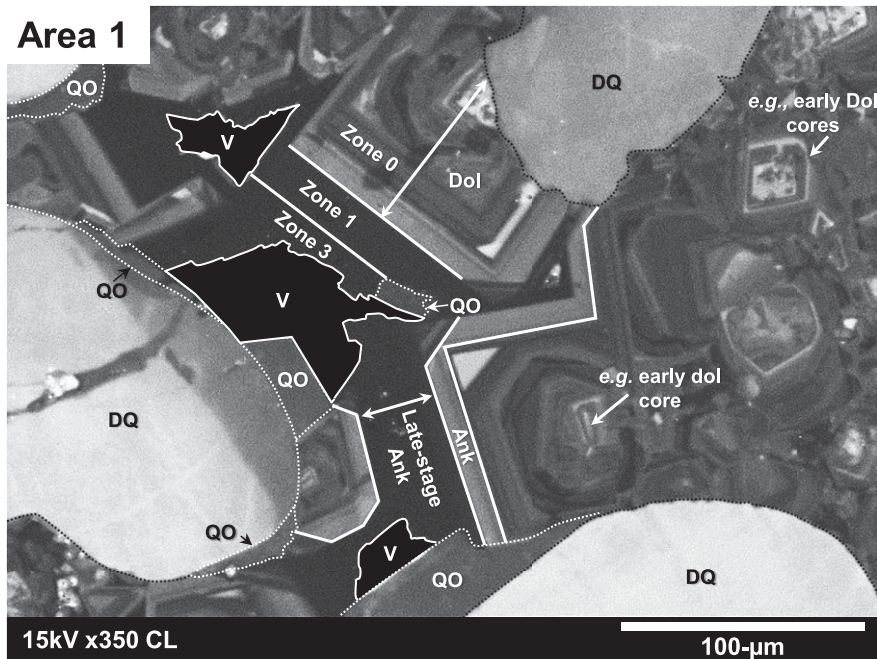


Figure A.1. Lithostratigraphy of core C131467 (Dane County, Wisconsin). Modified after Aswasereelert et al. (2008).

APPENDIX 3: PETROGRAPHIC DOCUMENTATION OF ALL SAMPLE REGIONS ANALYZED BY SECONDARY ION MASS SPECTROMETRY, WITH INDIVIDUALLY ANNOTATED ANALYSES PITS

(A) Area 1



(B) Area 9

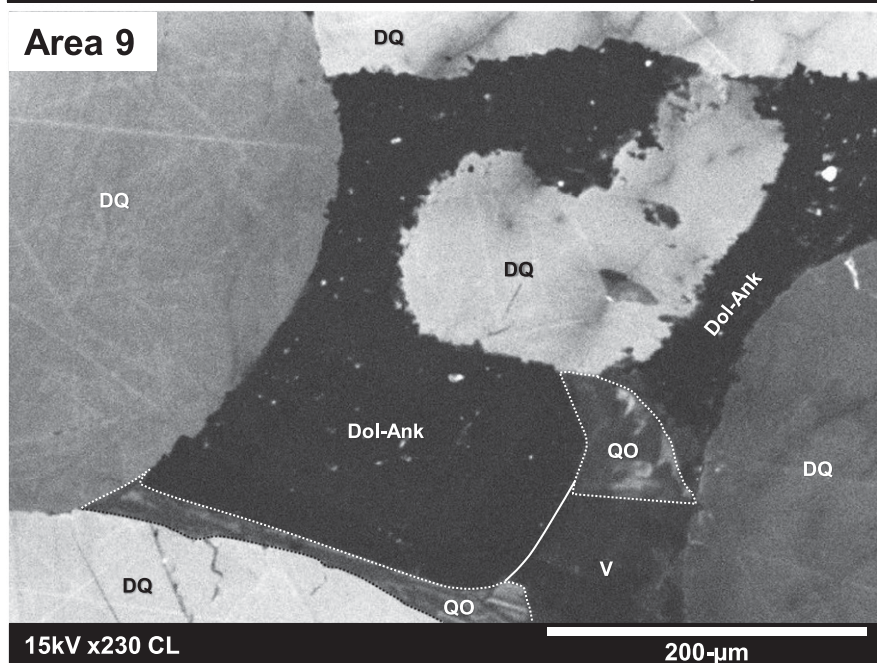


Plate 1. (A) Shaly sandstone sample SS-2 (northern Illinois): cathodoluminescence-scanning electron microscopy (CL-SEM) image that corresponds to the backscattered electron (BSE) image of Figure 4A in the main text (see also Plate 4A herein). (B) Shaly sandstone sample SS-3 (central Illinois): CL-SEM image that corresponds to the BSE image of Figure 4D in the main text (see also Plate 4A herein). Ank = ankerite; Cal = calcite; DF = detrital K-feldspar; Dol = dolomite; DQ = detrital quartz; OF = overgrowth K-feldspar; QO = quartz overgrowth; V = void space.

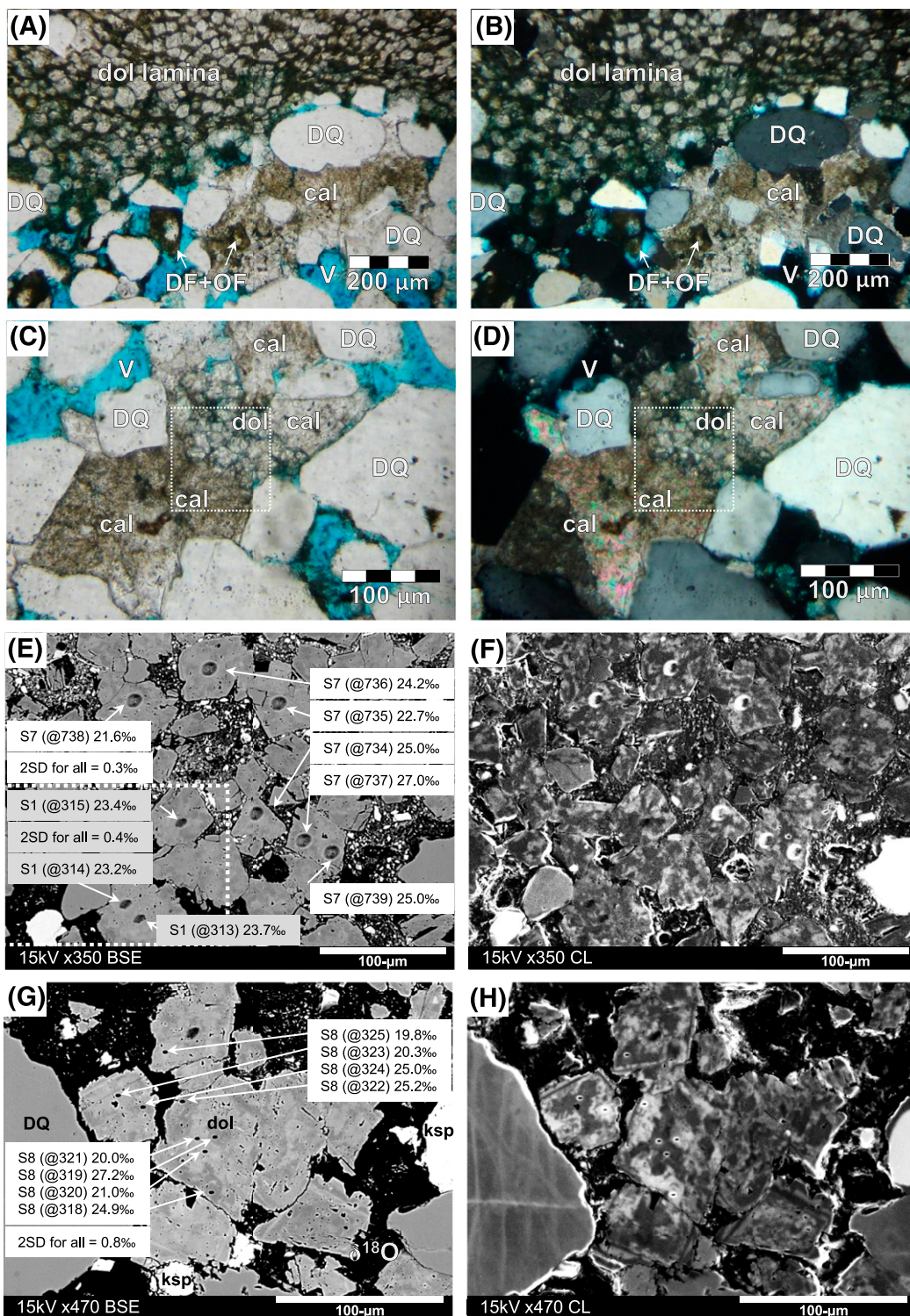


Plate 2. Characteristic morphologies of calcite and dolomite cements in shaly sandstone sample SS-1 (Wisconsin arch). (A, C) Photomicrographs in plane-polarized light with (B, D) corresponding cross-polarized light images. (E, G) Backscattered electron (BSE) images with annotated secondary ion mass spectrometry (SIMS) analysis pits ($\delta^{18}\text{O}$ Vienna standard mean ocean water [VSMOW]) and (F, H) corresponding cathodoluminescence (CL) images. Each analysis pit has a unique designation, such as “S8 (@205),” followed by the SIMS bias-corrected $\delta^{18}\text{O}$ (VSMOW) value and the two standard deviations (2SD) value in parentheses; the “S8” is an analytical session designator, whereas the “(@205)” is a unique sample pit identification number for the corresponding session. Refer to Table 2 in the main text and Appendices 1 and 2. Cal = calcite; DF = detrital K-feldspar; Dol = dolomite; DQ = detrital quartz; ksp = K-feldspar (DF+OF); OF = overgrowth K-feldspar; V = void space.

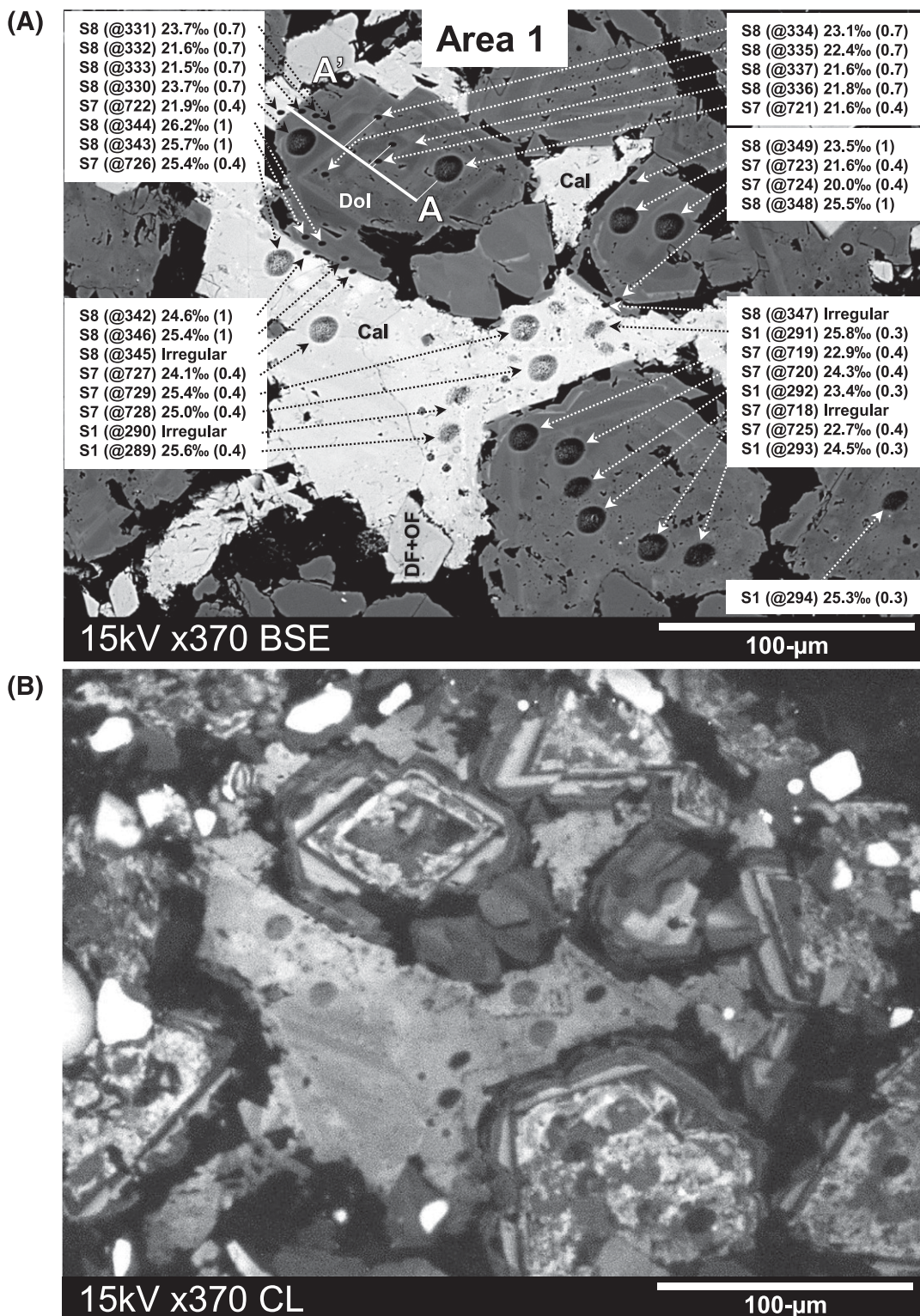


Plate 3. Shaly sandstone sample SS-1 (Wisconsin arch). (A) Backscattered electron (BSE) image of a representative sample region where the $\delta^{18}\text{O}$ Vienna standard mean ocean water (VSMOW) of carbonate cements (calcite and dolomite) was analyzed in situ by secondary ion mass spectrometry (SIMS). (B) Corresponding cathodoluminescence (CL) image. Each analysis pit has a unique designation, such as “S8 (@205),” followed by the SIMS bias-corrected $\delta^{18}\text{O}$ (VSMOW) value and the two standard deviations value in parentheses; the “S8” is an analytical session designator, whereas the “(@205)” is a unique sample pit identification number for the corresponding session. Refer to Table 2 in the main text and Appendices 1 and 2. Cal = calcite; DF = detrital K-feldspar; Dol = dolomite; OF = overgrowth K-feldspar.

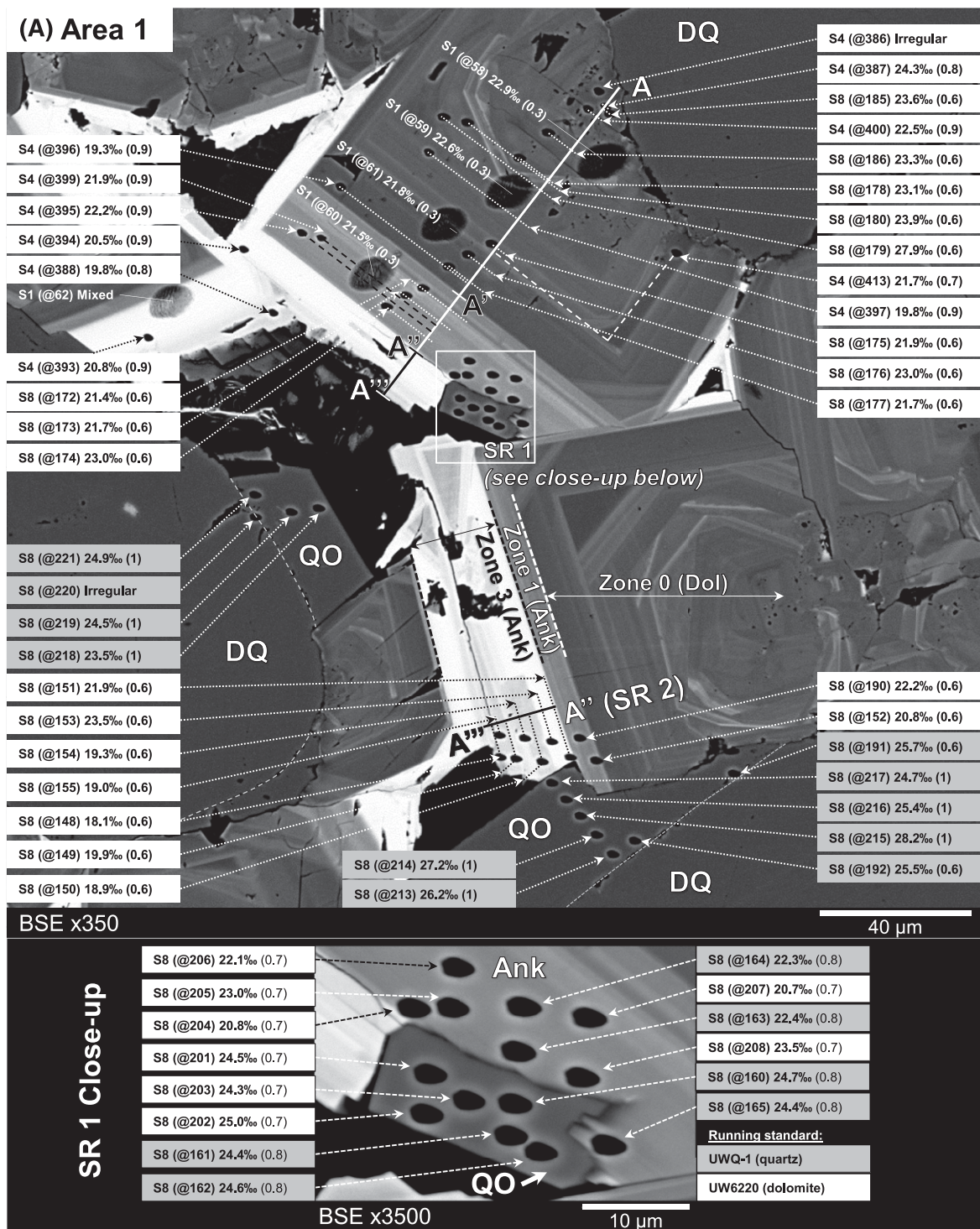
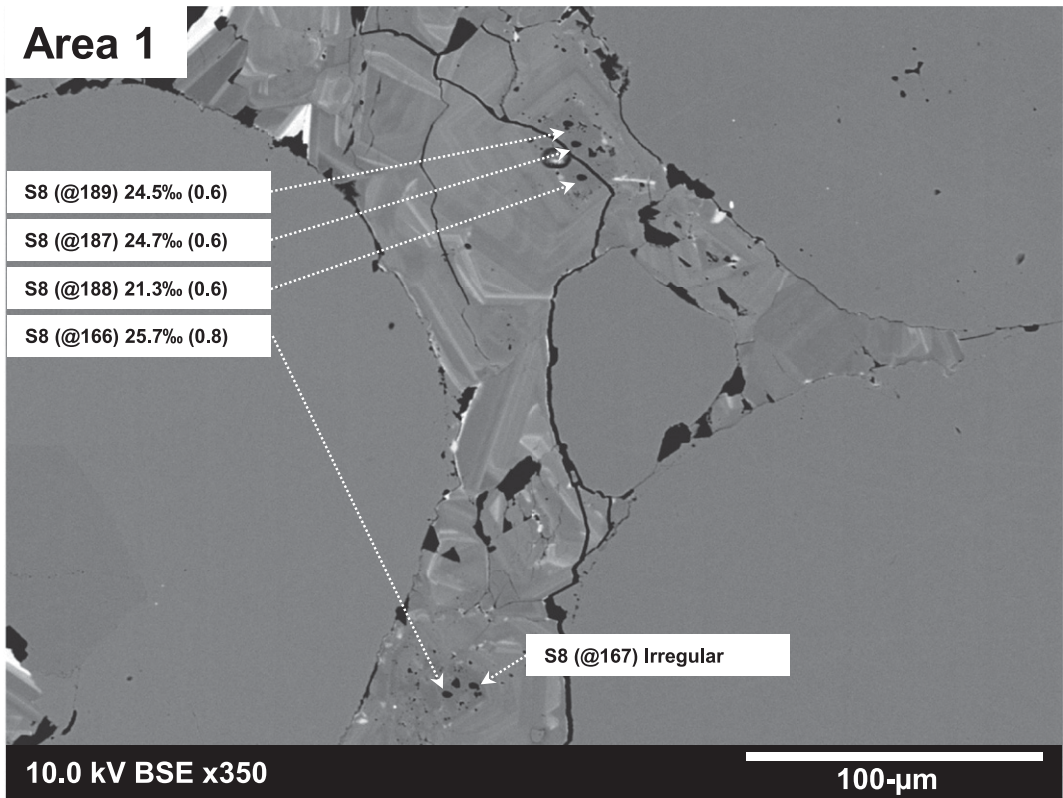


Plate 4. Shaly sandstone sample SS-2 (northern Illinois). (A) Backscattered electron (BSE) image of a representative sample region (Area 1) where the $\delta^{18}\text{O}$ Vienna standard mean ocean water (VSMOW) of all dolomite–ankerite cement generations was analyzed in situ by secondary ion mass spectrometry (SIMS). Refer to Plate 1A for corresponding cathodoluminescence (CL) image. (B) The BSE and (C) corresponding CL images of early dolomite cement and the placement of 3- μm SIMS spots within the innermost crystal cores. (D) The BSE image of a supplementary, representative region (Area 2) where dolomite–ankerite cements were analyzed. Each analysis pit has a unique designation, such as “S8 (@205),” followed by the SIMS bias-corrected $\delta^{18}\text{O}$ (VSMOW) value and the two standard deviations value in parentheses; the “S8” is an analytical session designator, whereas the “(@205)” is a unique sample pit identification number for the corresponding session. Refer to Table 2 in the main text and Appendices 1 and 2. Ank = ankerite; Dol = dolomite; DQ = detrital quartz; QO = quartz overgrowth; Sr = subregion.

(B)

Area 1



(C)

Area 1

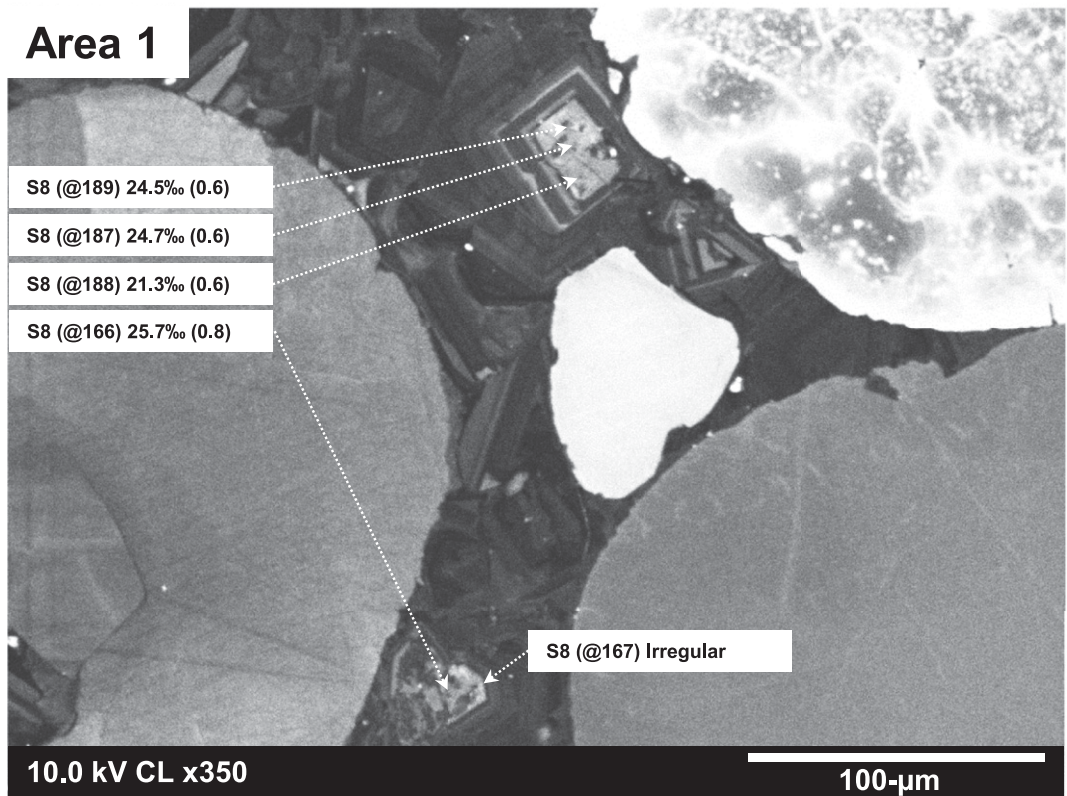


Plate 4. Continued.

(D)

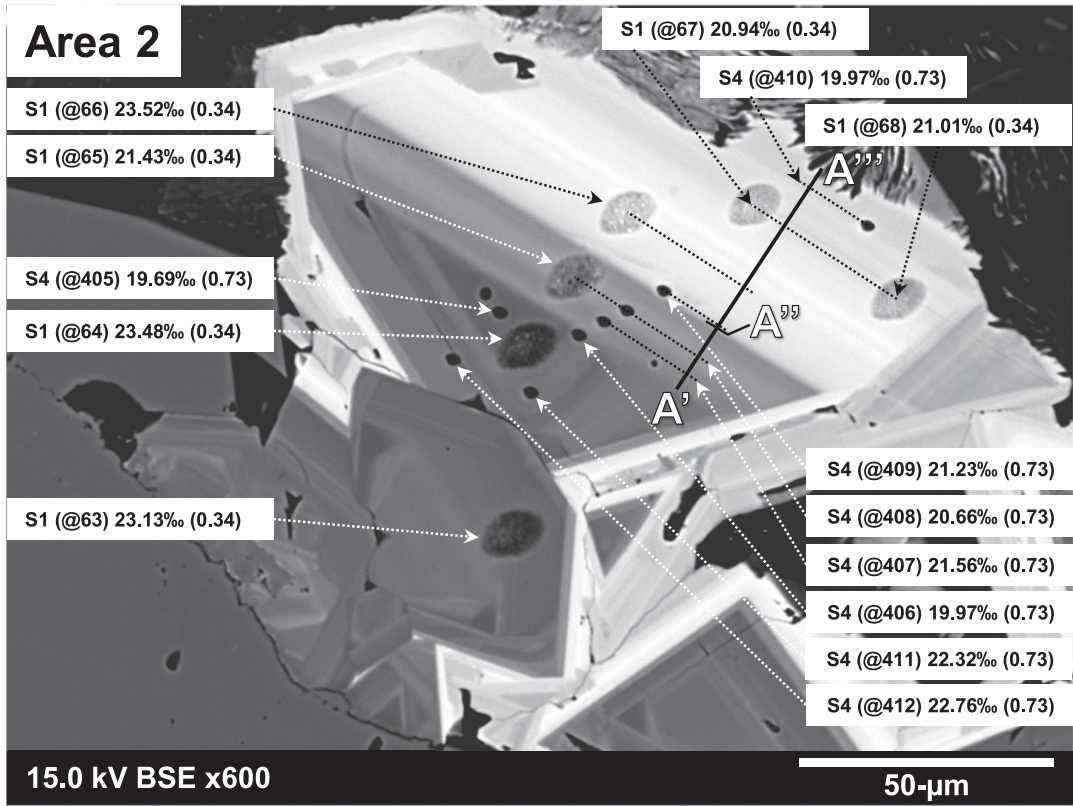


Plate 4. Continued.

(A)

Area 9

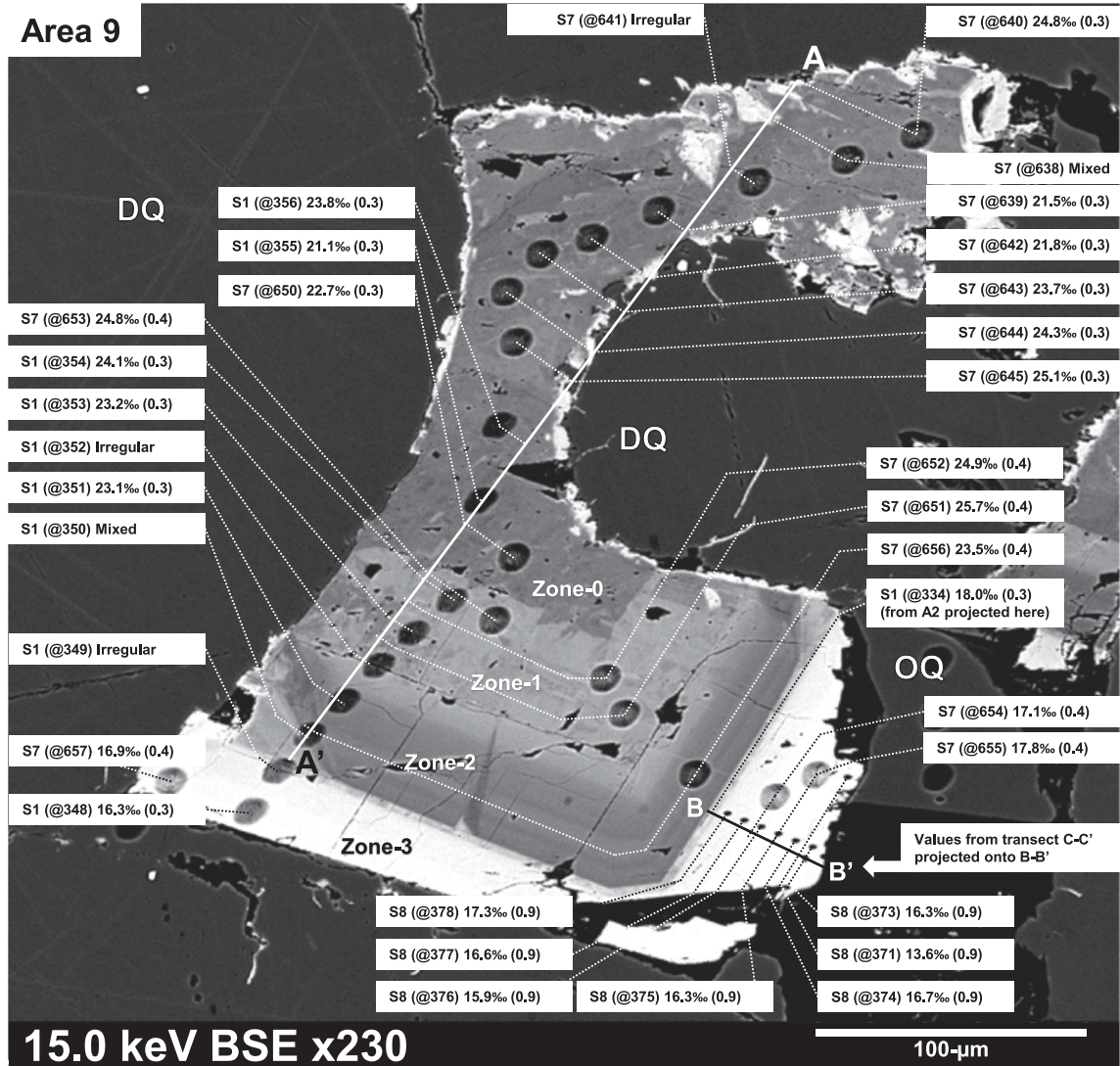


Plate 5. Shaly sandstone sample SS-3 (central Illinois). (A) Backscattered electron (BSE) image of a representative sample region (Area 9) where the $\delta^{18}\text{O}$ Vienna standard mean ocean water (VSMOW) of dolomite–ankerite cements was analyzed in situ by secondary ion mass spectrometry (SIMS). Refer to Plate 1B for corresponding cathodoluminescence image. (B, C) Additional regions analyzed (Areas 2 and 6, respectively). Each analysis pit has a unique designation, such as “S8 (@205),” followed by the SIMS bias-corrected $\delta^{18}\text{O}$ (VSMOW) value and the two standard deviations value in parentheses; the “S8” is an analytical session designator, whereas the “(@205)” is a unique sample pit identification number for the corresponding session. Refer to Table 2 in the main text and Appendices 1 and 2. Ank = ankerite; Dol = dolomite; DQ = detrital quartz; OQ = quartz overgrowth.

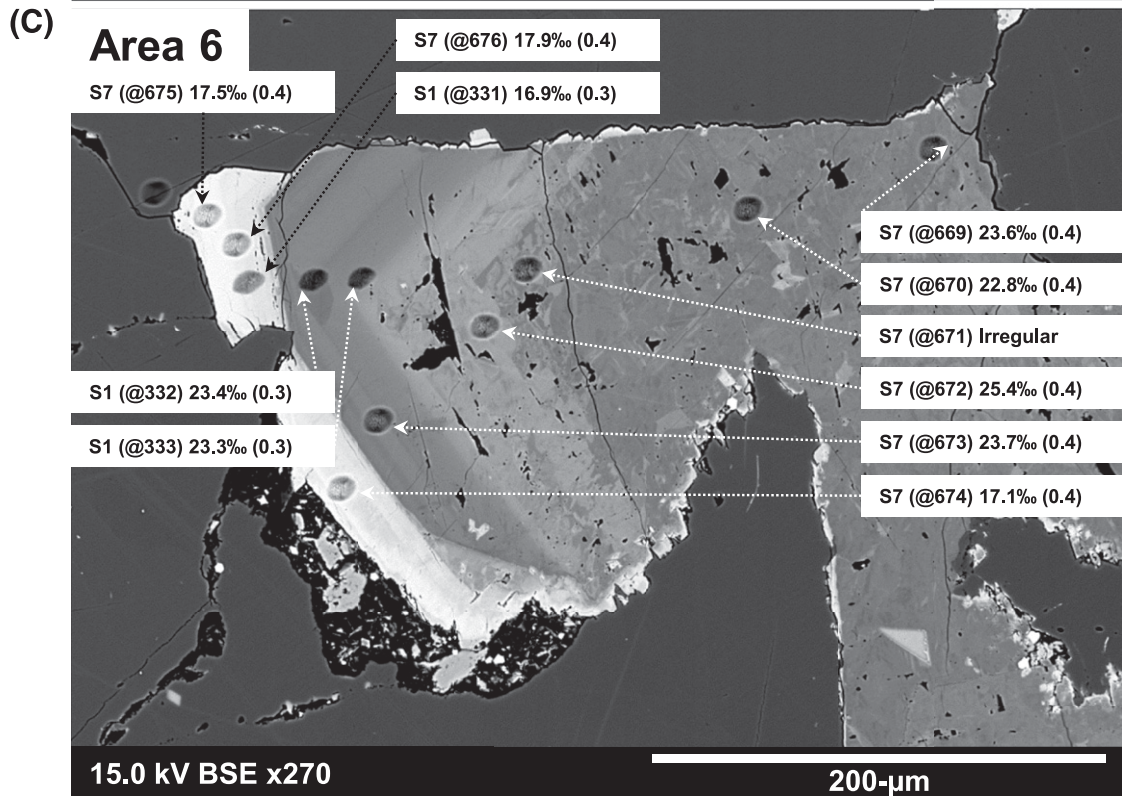
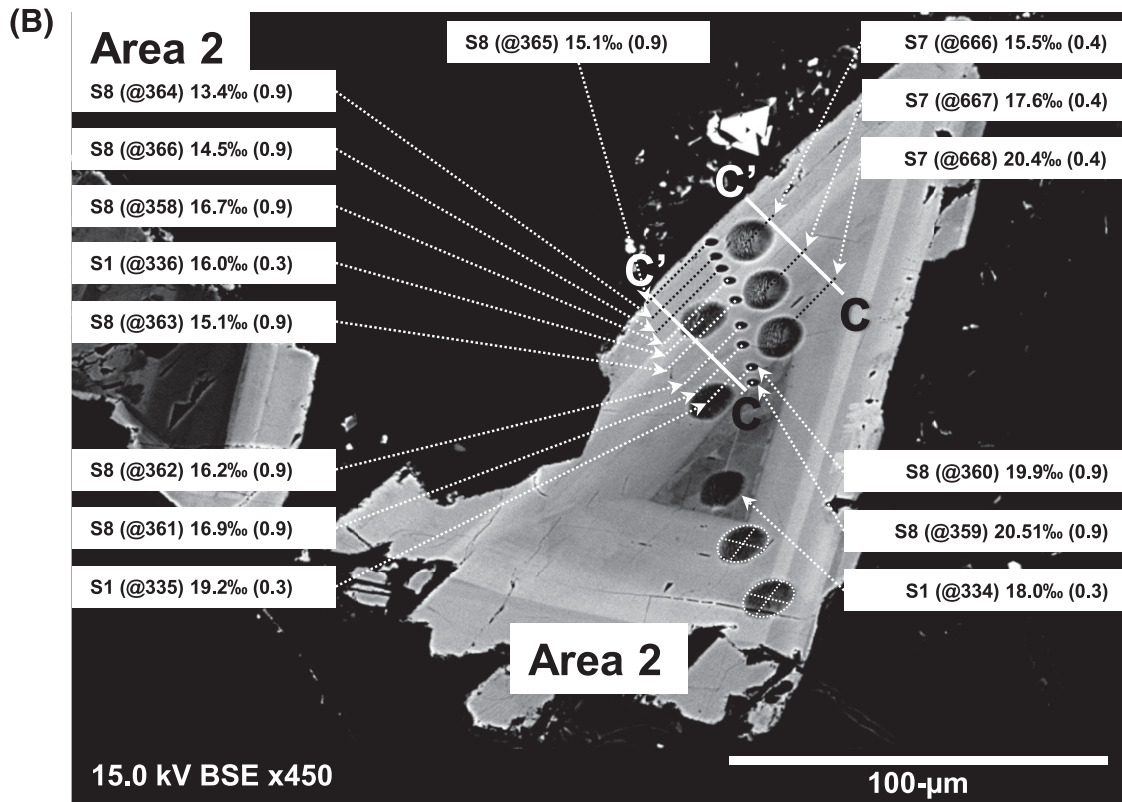


Plate 5. Continued.

APPENDIX 4: COMPLETE SECONDARY ION MASS SPECTROMETRY DATA TABLE: 10-µM SPOT-SIZE SESSIONS

SIIMS pit quality	Notes	File	Comment	$\delta^{18}\text{O}$ (‰, VSMOW)	2SD	$\delta^{18}\text{O}$ bias (‰, VSMOW)	$\delta^{18}\text{O}$ raw	$\delta^{18}\text{O}$ (2SE)	^{16}O (EB cps)	IP (nA)	Yield (E/Spot/nA)	date	time	X microns	Y microns	DTFA-X	DTFA-Y	$^{16}\text{O}/^{18}\text{O}$	Sample spot Fw# (Dot/Ank)	Sample spot Cw# (Cm/Dot)	
SIMS session S7 (10-µm spot-size): 13-16th May 2014																					
Calibration standard mount: WI-STD-80																					
		20140519@20.asc	UWC-3 Grain 4	8.02	0.39		8.02	0.39	1.837	1.190	1.628	5/14/2014	20:31	869	726	-21	-8	0.000878209	-	-	
		20140519@21.asc	UWC-3 Grain 1	7.88	0.36		7.88	0.36	1.815	1.174	1.631	5/14/2014	20:34	45	586	-21	-9	0.000918312	-	-	
		20140519@22.asc	UWC-3 Grain 2, Cs-res=183	7.74	0.42		7.74	0.42	2.045	1.234	1.657	5/14/2014	20:40	182	365	-19	-10	0.000804883	-	-	
		20140519@23.asc	UWC-3 Grain 3, Cs-res=183	7.81	0.41		7.81	0.41	2.060	1.244	1.656	5/14/2014	20:44	796	330	-19	-9	0.000871607	-	-	
			average and 2 SD	7.82	0.31		7.82	0.31													
		20140519@24.asc	UWO-1 grain 1	6.79	0.24		6.79	0.24	1.522	1.241	1.226	5/14/2014	20:49	484	1811	-26	-7	0.000319328	-	-	
		20140519@25.asc	UWO-1 grain 2	6.06	0.44		6.06	0.44	1.518	1.238	1.226	5/14/2014	20:53	388	2527	-26	-4	0.000285101	-	-	
		20140519@26.asc	UWO-1 grain 3	6.06	0.44		6.06	0.44	1.518	1.238	1.226	5/14/2014	20:57	388	2527	-26	-4	0.000285101	-	-	
		20140519@27.asc	UWO-1 grain 4	6.84	0.46		6.84	0.46	1.507	1.228	1.227	5/14/2014	21:00	10	4385	-29	4	0.000298573	-	-	
			average and 2 SD	6.87	0.25		6.87	0.25													
			bias*(STD-UW6220)	4.62																	
			Prop. error (2SE)	0.25																	
		20140519@28.asc	UW6220 dolomite Grain 1	12.40	0.28		12.40	0.28	2.180	1.219	1.788	5/14/2014	21:05	-1488	759	-22	-9	0.000860465	-	-	
		20140519@29.asc	UW6220 dolomite Grain 3	12.17	0.36		12.17	0.36	2.167	1.213	1.786	5/14/2014	21:09	-2532	1519	-23	-7	0.000918037	-	-	
		20140519@30.asc	UW6220 dolomite Grain 4	12.01	0.31		12.01	0.31	2.138	1.205	1.775	5/14/2014	21:12	-3654	1502	-24	9	0.000858085	-	-	
		20140519@31.asc	UW6220 dolomite Grain 2	12.03	0.32		12.03	0.32	2.163	1.194	1.762	5/14/2014	21:16	-2869	551	-22	-8	0.000902639	-	-	
			average and 2 SD	12.41	0.37		12.41	0.37													
			bias*(STD-UW6220)	0.00																	
			Prop. error (2SE)	0.23																	
		20140519@32.asc	UWARK1 Grain 3	13.86	0.17		13.86	0.17	2.210	1.178	1.879	5/14/2014	21:23	-1215	-2275	-16	-10	0.001079286	-	-	
		20140519@33.asc	UWARK1 Grain 5	13.76	0.17		13.76	0.17	2.181	1.162	1.878	5/14/2014	21:27	-1221	-4085	-14	-13	0.00118702	-	-	
		20140519@34.asc	UWARK1 Grain 2, Cs-res=184	7.89	0.44		7.89	0.44	1.848	1.187	1.641	5/14/2014	21:50	-38	-300	-17	-11	0.000970959	-	-	
		20140519@35.asc	UWARK1 Grain 3	7.64	0.38		7.64	0.38	1.951	1.187	1.643	5/14/2014	21:53	962	-300	-16	-11	0.00096037	-	-	
			average and 2 SD	7.83	0.38		7.83	0.38													
			bias*(STD-UW6220)	8.12																	
			Prop. error (2SE)	0.28																	
		20140519@36.asc	UWC-3 Grain 4	8.09	0.47		8.09	0.47	1.864	1.151	1.619	5/14/2014	21:41	712	849	-19	-11	0.001160749	-	-	
		20140519@37.asc	UWC-3 Grain 1, Cs-res=184	7.82	0.43		7.82	0.43	1.861	1.187	1.619	5/14/2014	21:46	-70	377	-17	-11	0.000970959	-	-	
		20140519@38.asc	UWC-3 Grain 2	7.69	0.44		7.69	0.44	1.848	1.187	1.641	5/14/2014	21:50	-38	-300	-17	-11	0.00118142	-	-	
		20140519@39.asc	UWC-3 Grain 3	7.64	0.38		7.64	0.38	1.951	1.187	1.643	5/14/2014	21:53	962	-300	-16	-11	0.00096037	-	-	
			average and 2 SD	7.83	0.38		7.83	0.38													
			bias*(STD-UW6220)	5.41																	
			Prop. error (2SE)	0.23																	
SIMS $\delta^{18}\text{O}$ bias correction model for sample compositions along the dolomite-enferite solid solution series																					
		UW6220 dolomite		0.004																	
		UWARK1		0.522																	
				8.12																	
				$F = \frac{[Fe]/[Mg/Fe]}{[Ca]/[Mg/Ca]}$																	
				$bias_{\text{raw}} = \frac{(b_{\text{max}} * F) - b_{\text{min}}}{k} + x_{\text{raw}}$																	
				Session-specific constants:																	
				b_{min}	9.238																
				b_{max}	1.2																
				k	0.10																
				x = Fw/Ft = Fe/(Mg/Fe) molar ratio of analyzed sample spot																	
SIMS $\delta^{18}\text{O}$ bias correction model for sample compositions along the calcite-dolomite solid solution																					
		Standard		0.501																	
		UW6220 dolomite		0																	
		UWC-3 calcite		5.41																	
				$bias_{\text{raw}}(STD-UW6220) = 11.389x - 5.706$																	
				x = Ca/(Mg-Ca) molar ratio of analyzed sample spot																	
Data lines 20140519@377-433: sample data that is not the subject of this manuscript (ADM CCS#4: 5513.2 aka DW#41 5513.2)																					
Sample mount: C406: 3857																					
		20140519@384.asc	C406: 3857 UW6220: dol	12.08	0.33		12.08	0.33	2.923	1.270	1.929	5/16/2014	0:39	843	1105	-18	11	0.001375297	-	-	
		20140519@385.asc	C406: 3857 UW6220: dol	11.88	0.34		11.88	0.34	2.913	1.266	1.823	5/16/2014	0:42	943	1085	-18	12	0.002380406	-	-	
		20140519@386.asc	C406: 3857 UW6220: dol	12.07	0.30		12.07	0.30	2.296	1.266	1.814	5/16/2014	0:46	943	1085	-18	13	0.002058686	-	-	
		20140519@387.asc	C406: 3857 UW6220: dol	12.12	0.28		12.12	0.28	2.291	1.262	1.815	5/16/2014	0:49	943	1045	-17	13	0.002115155	-	-	
			average and 2 SD	12.04	0.21		12.04	0.21													
		20140519@388.asc	C406: 3857 AB Spot 1	19.99	0.35		19.99	0.35	2.959	1.262	1.869	5/16/2014	0:56	-541	4821	-2	10	0.003107776	-	-	
		20140519@389.asc	C406: 3857 AB Spot 2	16.60	0.25		16.60	0.25	2.397	1.256	1.908	5/16/2014	1:00	-611	4808	-3	10	0.002293844	-	-	
		20140519@390.asc	C406: 3857 AB Spot 3	19.89	0.23		19.89	0.23	2.358	1.252	1.864	5/16/2014	1:05	-517	4829	-3	10	0.002914289	-	-	
		20140519@391.asc	C406: 3857 AB Spot 4	18.77	0.21		18.77	0.21	2.946	1.246	1.863	5/16/2014	1:09	-577	4816	-2	9	0.003312042	-	-	
		20140519@392.asc	C406: 3857 AB Spot 5	17.56	0.31		17.56	0.31	2.942	1.246	1.863	5/16/2014	1:17	-656	4788	-3	9	0.002541469	-	-	
		20140519@393.asc	C406: 3857 AB Spot 6	16.75	0.27		16.75	0.27	2.942	1.236	1.865	5/16/2014	1:21	-671	4783	-3	9	0.002878145	-	-	
		20140519@394.asc	C406: 3857 AB Spot 7	19.39	0.23		19.39	0.23	2.942	1.234	1.867	5/16/2014	1:21	-671	4783	-3	9	0.002541469	-	-	
		20140519@395.asc	C406: 3857 AB Spot 8	20.18	0.20		20.18	0.20	2.216	1.230	1.863	5/16/2014	1:25	-687	4764	-3	9	0.002588852	-	-	
		20140519@396.asc	C406: 3857 UW6220: dol	11.88	0.33		11.88	0.33	2.168	1.210	1.792	5/16/2014	1:38	-924	1117	-20	14	0.002926952	-	-	
		20140519@397.asc	C406: 3857 UW6220: dol	12.39	0.28		12.39	0.28	2.140	1.202	1.780	5/16/2014	1:38	-924	1097	-19	15	0.002458731	-	-	
		20140519@398.asc	C406: 3857 UW6220: dol (Cs res. -> 211)	12.04	0.37		12.04	0.37	2.275	1.261	1.805	5/16/2014	1:38	-924	1077	-19	14	0.002275048	-	-	
		201405																			

Regular	Mixed analysis ¹⁰⁾ , usable	20130925@338.asc	C4006 3857 Area8 ROI 2 Spot 3	15.99	0.29	-0.86	15.11	0.23	1.887	0.986	1.914	9/25/2013 16:54	1729	3619	2	-12	2.863E-03	0.466
Irregular	Exclude: pit overlaps (cracks)	20130925@337.asc	C4006 3857 Area2 ROI 2 Spot 4	-	-	-	16.65	0.32	1.860	0.986	1.887	9/25/2013 16:59	1732	3558	4	-14	3.140E-03	-
Irregular	Exclude: pit overlaps (cracks)	20130925@338.asc	C4006 3857 Area2 ROI 2 Spot 5	-	-	-	15.06	0.31	1.886	0.983	1.919	9/25/2013 17:03	1737	3543	4	-13	5.136E-03	-
Regular	Mixed analysis (overlaps) + large cavity	20130925@340.asc	C4006 3857 Area2 ROI 2 Spot 2	-	-	-	17.52	0.30	1.832	0.974	1.880	9/25/2013 17:15	-1878	-1379	-1	-14	3.401E-03	-
Regular	Mixed analysis ¹⁰⁾ , usable	20130925@341.asc	C4006 3857 UWQ-1	12.33	-	-	7.78	0.37	0.967	1.257	1.287	9/25/2013 17:21	330	672	7	-13	5.761E-04	-
Irregular	Exclude: pit overlaps (cracks)	20130925@342.asc	C4006 3857 UWQ-1	-	-	-	7.85	0.38	1.208	0.980	1.258	9/25/2013 17:24	330	672	6	-14	5.877E-04	-
Irregular	Exclude: pit overlaps (cracks)	20130925@343.asc	C4006 3857 UWQ-1	-	-	-	7.52	0.33	1.203	0.985	1.259	9/25/2013 17:28	330	672	6	-14	5.897E-04	-
Regular	Mixed analysis (overlaps) + large cavity	20130925@344.asc	C4006 3857 UWQ-1	12.33	-	-	7.64	0.42	1.201	0.951	1.253	9/25/2013 17:31	330	622	-6	-14	5.959E-04	-
Regular	bracket average and 2SD			12.33	-	-	7.67	0.29										
Regular	Exclude: pit overlaps (cracks)	20130925@345.asc	Cs-Res=203	-	-	-	7.85	0.49	1.278	1.017	1.287	9/25/2013 17:41	385	622	-7	-14	5.887E-04	-
Irregular	Exclude: pit overlaps (cracks)	20130925@346.asc	C4006 3857 Area8 ROI 5 Spot 3	-	-	-	15.39	0.17	1.971	1.026	1.921	9/25/2013 17:45	-1865	-1852	0	-14	4.544E-03	-
Irregular	Exclude: pit overlaps (cracks)	20130925@347.asc	C4006 3857 Area8 ROI 5 Spot 4	-	-	-	15.70	0.25	1.984	1.029	1.938	9/25/2013 17:50	-1850	-1823	1	-14	3.468E-03	-
Irregular	Exclude: pit overlaps (cracks)	20130925@348.asc	C4006 3857 Area8 ROI 6 Spot 1	16.33	0.34	-0.95	15.37	0.28	1.966	1.032	1.906	9/25/2013 17:55	-550	-4974	-8	-5	3.276E-03	0.442
Irregular	Exclude: pit overlaps (cracks)	20130925@349.asc	C4006 3857 Area8 ROI 6 Spot 2	-	-	-	16.92	0.28	1.960	1.033	1.888	9/25/2013 17:59	-536	-4688	-8	-4	3.626E-03	-
Irregular	Exclude: pit overlaps (cracks)	20130925@350.asc	C4006 3857 Area8 ROI 6 Spot 4	-	-	-	19.96	0.28	1.928	1.029	1.873	9/25/2013 18:07	-510	-5011	-8	-5	3.126E-03	-
Irregular	Exclude: pit overlaps (cracks)	20130925@351.asc	C4006 3857 Area8 ROI 6 Spot 5	-	-	-	19.86	0.28	1.928	1.029	1.882	9/25/2013 18:11	-498	-5021	-7	-5	4.022E-03	-
Regular	Mixed analysis (overlaps) + large cavity	20130925@352.asc	C4006 3857 Area8 ROI 6 Spot 6	23.23	0.34	-1.98	21.44	0.29	1.913	1.020	1.876	9/25/2013 18:15	-482	-5033	-7	-5	3.429E-03	0.238
Regular	Mixed analysis (overlaps) + large cavity	20130925@353.asc	C4006 3857 Area8 ROI 6 Spot 7	24.07	0.34	-2.02	22.00	0.31	1.905	1.009	1.888	9/25/2013 18:20	-467	-5041	-7	-5	3.310E-03	0.233
Regular	Mixed analysis (overlaps) + large cavity	20130925@354.asc	C4006 3857 Area8 ROI 6 Spot 8	23.76	0.34	-1.94	20.53	0.25	1.893	0.980	1.892	9/25/2013 18:24	-442	-5078	-7	-5	3.445E-03	0.136
Regular	Mixed analysis (overlaps) + large cavity	20130925@355.asc	C4006 3857 Area8 ROI 6 Spot 9	23.76	0.34	-3.15	20.53	0.25	1.893	0.980	1.912	9/25/2013 18:27	-442	-5108	-7	-5	3.288E-03	0.143
Regular	Mixed analysis (overlaps) + large cavity	20130925@357.asc	C4006 3857 UWQ-1	12.33	-	-	7.62	0.40	1.254	0.985	1.273	9/25/2013 18:33	254	704	-5	-13	6.008E-04	-
Regular	Mixed analysis (overlaps) + large cavity	20130925@358.asc	C4006 3857 UWQ-1	-	-	-	7.62	0.47	1.250	0.987	1.266	9/25/2013 18:36	254	684	-5	-14	5.899E-04	-
Regular	Mixed analysis (overlaps) + large cavity	20130925@359.asc	C4006 3857 UWQ-1	-	-	-	7.45	0.45	1.245	0.983	1.267	9/25/2013 18:40	254	684	-5	-14	5.970E-04	-
Regular	Mixed analysis (overlaps) + large cavity	20130925@360.asc	C4006 3857 UWQ-1	-	-	-	7.47	0.54	1.245	0.986	1.268	9/25/2013 18:43	254	684	-5	-15	5.963E-04	-
Regular	bracket average and 2SD			12.33	-	-	7.66	0.34										
Regular	Mixed analysis ¹⁰⁾ , usable	20130925@361.asc	C4006 3857 Area8 ROI 3 Spot 1	15.22	0.53	-0.67	14.54	0.23	1.984	0.972	1.989	9/25/2013 18:48	2765	3890	5	-12	3.268E-03	0.464
Irregular	Exclude: pit overlaps (cracks)	20130925@362.asc	C4006 3857 Area8 ROI 3 Spot 2	-	-	-	18.83	0.23	1.879	0.972	1.934	9/25/2013 18:52	2175	3890	-5	-11	3.295E-03	-
Irregular	Exclude: pit overlaps (cracks)	20130925@363.asc	C4006 3857 Area8 ROI 3 Spot 3	-	-	-	19.92	0.35	1.879	0.972	1.934	9/25/2013 18:56	2175	3882	-5	-13	3.295E-03	-
Irregular	Exclude: pit overlaps (cracks)	20130925@364.asc	C4006 3857 Area8 ROI 3 Spot 4	-	-	-	22.89	0.20	1.885	0.967	1.919	9/25/2013 19:01	2151	3882	-5	-12	3.389E-03	-
Irregular	Exclude: pit overlaps (cracks)	20130925@365.asc	C4006 3857 Area8 ROI 3 Spot 5	-	-	-	20.64	0.34	1.885	0.968	1.930	9/25/2013 19:05	2134	3877	-5	-12	3.262E-03	-
Regular	Imagewrite + mixed analysis ¹⁰⁾ , exclude	20130925@366.asc	C4006 3857 Area8 ROI 3 Spot 6	23.39	0.53	-2.98	20.34	0.31	1.875	0.977	1.919	9/25/2013 19:09	2126	3885	-6	-12	3.112E-03	0.141
Regular	Exclude: pit overlaps (cracks)	20130925@367.asc	C4006 3857 Area8 ROI 3 Spot 7	-	-	-	19.91	0.27	1.882	0.981	1.919	9/25/2013 19:13	1684	3902	-6	-10	3.445E-03	-
Regular	Exclude: pit overlaps (cracks)	20130925@368.asc	C4006 3857 Area8 ROI 3 Spot 8	-	-	-	19.91	0.27	1.882	0.981	1.919	9/25/2013 19:18	1684	3902	-6	-11	3.445E-03	-
Regular	Exclude: pit overlaps (cracks)	20130925@369.asc	C4006 3857 Area8 ROI 3 Spot 9	24.34	0.53	-1.76	22.54	0.33	1.859	0.979	1.898	9/25/2013 19:23	2165	3907	-5	-11	3.389E-03	0.238
Regular	Mixed analysis ¹⁰⁾ , usable	20130925@370.asc	C4006 3857 UWQ-1	12.33	-	-	8.04	0.51	1.222	0.981	1.246	9/25/2013 19:29	236	703	-5	-13	5.900E-04	-
Irregular	Exclude: pit overlaps (cracks)	20130925@371.asc	C4006 3857 UWQ-1	-	-	-	8.08	0.32	1.216	0.979	1.241	9/25/2013 19:37	160	702	-5	-13	6.337E-04	-
Irregular	Exclude: pit overlaps (cracks)	20130925@372.asc	C4006 3857 UWQ-1	-	-	-	7.89	0.33	1.219	0.976	1.249	9/25/2013 19:41	160	682	-5	-15	6.230E-04	-
Regular	Mixed analysis (overlaps) + large cavity	20130925@373.asc	C4006 3857 UWQ-1	12.33	-	-	8.560	0.49	1.218	0.973	1.253	9/25/2013 19:45	160	662	-5	-14	6.200E-04	-
Regular	bracket average and 2SD			12.33	-	-	8.07	0.33										
Regular	bracket average and 2SD			12.33	-	-	7.87	0.53										

¹⁰⁾ **Mixed analysis:** In the *in-situ* analysis of $\delta^{18}\text{O}$ in chemically zoned carbonate minerals by SIMS, it is preferable that each sample pit be placed within a single compositional zone (avoiding overlaps) if the width of individual zones can accommodate the commonly used 10- μm -diameter spot-size. In the application of SIMS $\delta^{18}\text{O}$ *data* corrections, this minimizes the component of uncertainty that is functionally related to the cation-composition ($\text{Fe}^{2+} = \text{Fe}/(\text{Mg} + \text{Fe})$) of the analyzed sample spot. *Data* corrections cannot be confidently applied in instances where a pit overlaps two or more zones; this is because the pit geometry cannot easily be modeled as a simple symmetric ellipsoid, and thus it is difficult to accurately assess the contribution of each zone to the total volume of spattered sample material. Such mixed analyses are typically excluded from data compilations unless the extent of overlap is minor (<3%, based on the surface footprint of the SIMS pit) and the compositional contrast between the relevant zones (based on BSE-SEM imaging) is not visually striking. Mixed analysis pits are thus either labeled as "Mixed analysis (excluded)" or "Mixed analysis (usable)".

Regular	C12986 1217.3 A1 R1 Spot10 Do-Ank	21.89	0.93	-17.83	3.56	0.39	53.087	2/27/2014 19:12	-876	-1795	-11	-18	2.802E-03
Regular	C12986 1217.3 A1 R1 Spot11 Do-Ank	22.54	0.93	-24.12	-2.13	0.37	43.316	2/27/2014 19:22	-908	-1756	-9	-18	5.671E-03
	Bracket: average and 2SD												
	C12986 1217.3 UWO-1	12.33	0.50	-6.09	0.50	0.50	35.221	2/27/2014 19:32	132	460	-13	-10	7.915E-04
	C12986 1217.3 UWO-1	12.33	0.50	-6.04	0.49	0.50	34.559	2/27/2014 19:40	137	460	-14	-10	8.294E-04
	C12986 1217.3 UWO-1	12.33	0.50	-6.55	0.65	0.57	34.581	2/27/2014 19:54	151	460	-14	-10	8.039E-04
	Bracket: average and 2SD												
	C12986 1217.3 A2 R2 Spot1 Do-Ank	19.69	0.73	-24.24	-5.02	0.51	44.582	2/27/2014 20:05	-1468	-2732	-3	-24	2.935E-03
	C12986 1217.3 A2 R2 Spot2 Do-Ank	19.57	0.73	-21.18	-1.63	0.53	46.153	2/27/2014 20:13	-1453	-2786	-3	-25	2.813E-03
	C12986 1217.3 A2 R2 Spot3 Do-Ank	21.56	0.73	-18.77	2.38	0.48	50.366	2/27/2014 20:21	-1451	-2795	-3	-25	2.835E-03
	C12986 1217.3 A2 R2 Spot4 Do-Ank	21.23	0.73	-16.66	4.22	0.46	52.780	2/27/2014 20:36	-1437	-2788	-3	-26	2.867E-03
	C12986 1217.3 A2 R2 Spot5 Do-Ank	19.97	0.73	-16.67	2.86	0.46	59.572	2/27/2014 20:43	-1401	-2775	-5	-25	2.807E-03
	C12986 1217.3 A2 R2 Spot6 Do-Ank	22.32	0.73	-22.02	-0.19	0.60	46.590	2/27/2014 20:52	-1465	-2807	-4	-25	3.090E-03
	C12986 1217.3 A2 R2 Spot7 Do-Ank	22.76	0.73	-21.44	0.83	0.41	47.189	2/27/2014 21:00	-1477	-2803	-4	-23	4.741E-03
	C12986 1217.3 A1 R1 Spot8 Do-Ank	21.68	0.73	-24.82	-3.76	0.66	44.068	2/27/2014 21:09	-1767	-1752	-5	-20	3.149E-03
	Bracket: average and 2SD												
	C12986 1217.3 UWO-1	12.33	0.55	-6.12	0.55	0.55	34.155	2/27/2014 21:20	131	450	-5	-12	7.872E-04
	C12986 1217.3 UWO-1	12.33	0.55	-6.09	0.57	0.57	33.725	2/27/2014 21:27	138	450	-5	-13	7.989E-04
	C12986 1217.3 UWO-1	12.33	0.55	-7.308	0.85	0.60	34.079	2/27/2014 21:34	145	450	-5	-12	8.195E-04
	C12986 1217.3 UWO-1	12.33	0.55	-6.56	0.55	0.55	34.582	2/27/2014 21:48	159	458	-4	-10	7.832E-04
	Bracket: average and 2SD												
	C12986 1217.3 UWO-1	12.33	0.86	-6.21	0.86	0.86	34.582	2/27/2014 21:48	159	458	-4	-10	7.832E-04
	Bracket: average and 2SD												
	C12986 1217.3 UWO-1	12.33	0.86	-6.18	0.73	0.73	34.582	2/27/2014 21:48	159	458	-4	-10	7.832E-04

SIMS session S8 (3-µm spot-size): 22-25th July, 2014

Calibration standard mount: WI-STD-80

Regular	WI-STD-80 UWC-3 SW gr	0.00	0.63	-7.92	0.53	0.53	45.191	7/22/2014 17:49	68	-481	5 <th>-4</th> <th>0.01916663</th>	-4	0.01916663
Regular	WI-STD-80 UWC-3 gr.1	0.00 <th>0.61</th> <th>-8.09</th> <th>0.61</th> <th>0.61</th> <th>44.952</th> <th>7/22/2014 17:57</th> <th>-301</th> <th>311</th> <th>5</th>	0.61	-8.09	0.61	0.61	44.952	7/22/2014 17:57	-301	311	5	4	0.01891053
Regular	WI-STD-80 UWC-3 gr.4	0.00 <th>0.68</th> <th>-7.46</th> <th>0.68</th> <th>0.68</th> <th>44.688</th> <th>7/22/2014 18:05</th> <th>883</th> <th>602</th>	0.68	-7.46	0.68	0.68	44.688	7/22/2014 18:05	883	602	4 <th>-4</th> <th>0.01912977</th>	-4	0.01912977
Regular	WI-STD-80 UWC-3 gr.5	0.00 <th>0.73</th> <th>-8.06</th> <th>0.73</th> <th>0.73</th> <th>44.420</th> <th>7/22/2014 18:13</th> <th>672</th> <th>-139</th> <th>4</th>	0.73	-8.06	0.73	0.73	44.420	7/22/2014 18:13	672	-139	4	-5	0.01865595
	average and 2SD												
Regular	WI-STD-80 UW6220 gr.1	15.88	0.46	-3.74	0.46	0.46	43.136	7/22/2014 18:21 <th>-1422</th> <th>938</th> <th>4 <th>-5</th> <th>0.0202446</th> </th>	-1422	938	4 <th>-5</th> <th>0.0202446</th>	-5	0.0202446
Regular	WI-STD-80 UW6220 gr.3	15.88	0.57	-3.93	0.57	0.57	43.737	7/22/2014 18:29 <th>-2434</th> <th>1537</th> <th>4 <th>-5</th> <th>0.01902186</th> </th>	-2434	1537	4 <th>-5</th> <th>0.01902186</th>	-5	0.01902186
Regular	WI-STD-80 UW6220 gr.4	15.88	0.49	-3.33	0.49	0.49	43.203	7/22/2014 18:36 <th>-3653</th> <th>1670</th> <th>4 <th>-5</th> <th>0.01842389</th> </th>	-3653	1670	4 <th>-5</th> <th>0.01842389</th>	-5	0.01842389
Regular	WI-STD-80 UW6220 gr.5	15.88	0.59	-3.78	0.59	0.59	44.306	7/22/2014 18:45 <th>-3527</th> <th>2487</th> <th>3 <th>-5</th> <th>0.01927119</th> </th>	-3527	2487	3 <th>-5</th> <th>0.01927119</th>	-5	0.01927119
	average and 2SD												
	bias(STD-UW6220)	0.00											
	Prop. error (2SE):	0.00											
	bias(STD-UWC-1)	0.00											
	Prop. error (2SE):	0.43											
	bias(STD-UWC-3)	0.00											
	Prop. error (2SE):	0.43											
	bias(STD-UWC-4)	0.00											
	Prop. error (2SE):	0.43											
	bias(STD-UWC-5)	0.00											
	Prop. error (2SE):	0.43											
	bias(STD-UWC-6)	0.00											
	Prop. error (2SE):	0.43											
	bias(STD-UWC-7)	0.00											
	Prop. error (2SE):	0.43											
	bias(STD-UWC-8)	0.00											
	Prop. error (2SE):	0.43											
	bias(STD-UWC-9)	0.00											
	Prop. error (2SE):	0.43											
	bias(STD-UWC-10)	0.00											
	Prop. error (2SE):	0.43											
	bias(STD-UWC-11)	0.00											
	Prop. error (2SE):	0.43											
	bias(STD-UWC-12)	0.00											
	Prop. error (2SE):	0.43											
	bias(STD-UWC-13)	0.00											
	Prop. error (2SE):	0.43											
	bias(STD-UWC-14)	0.00											
	Prop. error (2SE):	0.43											
	bias(STD-UWC-15)	0.00											
	Prop. error (2SE):	0.43											
	bias(STD-UWC-16)	0.00											
	Prop. error (2SE):	0.43											
	bias(STD-UWC-17)	0.00											
	Prop. error (2SE):	0.43											
	bias(STD-UWC-18)	0.00											
	Prop. error (2SE):	0.43											
	bias(STD-UWC-19)	0.00											
	Prop. error (2SE):	0.43											
	bias(STD-UWC-20)	0.00											
	Prop. error (2SE):	0.43											
	bias(STD-UWC-21)	0.00											
	Prop. error (2SE):	0.43											
	bias(STD-UWC-22)	0.00											
	Prop. error (2SE):	0.43											
	bias(STD-UWC-23)	0.00											
	Prop. error (2SE):	0.43											
	bias(STD-UWC-24)	0.00											
	Prop. error (2SE):	0.43											
	bias(STD-UWC-25)	0.00											
	Prop. error (2SE):	0.43											
	bias(STD-UWC-26)	0.00											
	Prop. error (2SE):	0.43											
	bias(STD-UWC-27)	0.00											
	Prop. error (2SE):	0.43											
	bias(STD-UWC-28)	0.00											
	Prop. error (2SE):	0.43											
	bias(STD-UWC-29)	0.00											
	Prop. error (2SE):	0.43											
	bias(STD-UWC-30)	0.00											
	Prop. error (2SE):	0.43											
	bias(STD-UWC-31)	0.00											
	Prop. error (2SE):	0.43											
	bias(STD-UWC-32)	0.00											
	Prop. error (2SE):	0.43											
	bias(STD-UWC-33)	0.00											
	Prop. error (2SE):	0.43											
	bias(STD-UWC-34)	0.00											
	Prop. error (2SE):	0.43											
	bias(STD-UWC-35)	0.00											
	Prop. error (2SE):	0.43											
	bias(STD-UWC-36)	0.00											
	Prop. error (2SE):	0.43											
	bias(STD-UWC-37)	0.00											
	Prop. error (2SE):	0.43											
	bias(STD-UWC-38)	0.00											
	Prop. error (2SE):	0.43											
	bias(STD-UWC-39)	0.00											
	Prop. error (2SE):	0.43											

Calibration standard mount: 2014_MGS_Carb_02

Sample	Standard	Fe# = $\frac{[Fe]}{[Mg+Fe]}$	$\frac{bias*(STD-UW6220)}{k}$	Prep. error (ZSE):
20140722@46.asc	2014_MGS_Carb_02 UW6220	0.55	0.00	8.27
20140722@47.asc	2014_MGS_Carb_02 UW6220	0.55	0.00	0.64
20140722@48.asc	2014_MGS_Carb_02 UW6220	0.55	0.00	
20140722@49.asc	2014_MGS_Carb_02 UW6220	0.55	0.00	
20140722@50.asc	2014_MGS_Carb_02 UW6220	0.55	0.00	
20140722@51.asc	2014_MGS_Carb_02 UW6220	0.55	0.00	
20140722@52.asc	2014_MGS_Carb_02 UW6220	0.55	0.00	
20140722@53.asc	2014_MGS_Carb_02 UW6220	0.55	0.00	
20140722@54.asc	2014_MGS_Carb_02 UW6220	0.55	0.00	
20140722@55.asc	2014_MGS_Carb_02 UW6220	0.55	0.00	
20140722@56.asc	2014_MGS_Carb_02 UW6220	0.55	0.00	
20140722@57.asc	2014_MGS_Carb_02 UW6220	0.55	0.00	
20140722@58.asc	2014_MGS_Carb_02 UW6220	0.55	0.00	
20140722@59.asc	2014_MGS_Carb_02 UW6220	0.55	0.00	
20140722@60.asc	2014_MGS_Carb_02 UW6220	0.55	0.00	
20140722@61.asc	2014_MGS_Carb_02 UW6220	0.55	0.00	
20140722@62.asc	2014_MGS_Carb_02 UW6220	0.55	0.00	
20140722@63.asc	2014_MGS_Carb_02 UW6220	0.55	0.00	
20140722@64.asc	2014_MGS_Carb_02 UW6220	0.55	0.00	
20140722@65.asc	2014_MGS_Carb_02 UW6220	0.55	0.00	
20140722@66.asc	2014_MGS_Carb_02 UW6220	0.55	0.00	
20140722@67.asc	2014_MGS_Carb_02 UW6220	0.55	0.00	
20140722@68.asc	2014_MGS_Carb_02 UW6220	0.55	0.00	
20140722@69.asc	2014_MGS_Carb_02 UW6220	0.55	0.00	
20140722@70.asc	2014_MGS_Carb_02 UW6220	0.55	0.00	
20140722@71.asc	2014_MGS_Carb_02 UW6220	0.55	0.00	
20140722@72.asc	2014_MGS_Carb_02 UW6220	0.55	0.00	
20140722@73.asc	2014_MGS_Carb_02 UW6220	0.55	0.00	
20140722@74.asc	2014_MGS_Carb_02 UW6220	0.55	0.00	
20140722@75.asc	2014_MGS_Carb_02 UW6220	0.55	0.00	
20140722@76.asc	2014_MGS_Carb_02 UW6220	0.55	0.00	
20140722@77.asc	2014_MGS_Carb_02 UW6220	0.55	0.00	
20140722@78.asc	2014_MGS_Carb_02 UW6220	0.55	0.00	
20140722@79.asc	2014_MGS_Carb_02 UW6220	0.55	0.00	
20140722@80.asc	2014_MGS_Carb_02 UW6220	0.55	0.00	
20140722@81.asc	2014_MGS_Carb_02 UW6220	0.55	0.00	
20140722@82.asc	2014_MGS_Carb_02 UW6220	0.55	0.00	
20140722@83.asc	2014_MGS_Carb_02 UW6220	0.55	0.00	
20140722@84.asc	2014_MGS_Carb_02 UW6220	0.55	0.00	
20140722@85.asc	2014_MGS_Carb_02 UW6220	0.55	0.00	
20140722@86.asc	2014_MGS_Carb_02 UW6220	0.55	0.00	
20140722@87.asc	2014_MGS_Carb_02 UW6220	0.55	0.00	
20140722@88.asc	2014_MGS_Carb_02 UW6220	0.55	0.00	
20140722@89.asc	2014_MGS_Carb_02 UW6220	0.55	0.00	
20140722@90.asc	2014_MGS_Carb_02 UW6220	0.55	0.00	
20140722@91.asc	2014_MGS_Carb_02 UW6220	0.55	0.00	
20140722@92.asc	2014_MGS_Carb_02 UW6220	0.55	0.00	
20140722@93.asc	2014_MGS_Carb_02 UW6220	0.55	0.00	
20140722@94.asc	2014_MGS_Carb_02 UW6220	0.55	0.00	
20140722@95.asc	2014_MGS_Carb_02 UW6220	0.55	0.00	
20140722@96.asc	2014_MGS_Carb_02 UW6220	0.55	0.00	
20140722@97.asc	2014_MGS_Carb_02 UW6220	0.55	0.00	
20140722@98.asc	2014_MGS_Carb_02 UW6220	0.55	0.00	
20140722@99.asc	2014_MGS_Carb_02 UW6220	0.55	0.00	
20140722@100.asc	2014_MGS_Carb_02 UW6220	0.55	0.00	

SIMS ⁵⁷Fe bias correction model for sample compositions along the dolomite-ankerite solid solution series

$$Fe\# = \frac{[Fe]}{[Mg+Fe]}$$

$$bias*(STD-UW6220) = \frac{bias*(STD-UW6220)}{k}$$

$$bias*(STD-UW6220) = \frac{bias*(STD-UW6220)}{k}$$

Session-specific constants:

$$bias_{max} = 10.98$$

$$n = 1.2$$

$$k = 0.10$$

x = Fe# (Fe/(Mg+Fe)) molar ratio of analyzed sample spot

Sample mount: C12996 1217.3

Standard: UW6220 160omite

UWank1 9.31

UWank4 8.27

average and ZSD

22.60

22.60

22.60

22.60

22.60

22.60

22.60

22.60

22.60

22.60

22.60

22.60

22.60

22.60

22.60

22.60

22.60

22.60

22.60

22.60

22.60

22.60

22.60

22.60

22.60

22.60

22.60

22.60

22.60

22.60

22.60

22.60

22.60

22.60

22.60

22.60

22.60

22.60

22.60

22.60

22.60

22.60

22.60

22.60

22.60

22.60

22.60

22.60

22.60

22.60

22.60

22.60

22.60

22.60

22.60

22.60

22.60

22.60

22.60

22.60

22.60

22.60

22.60

22.60

22.60

22.60

22.60

22.60

22.60

22.60

22.60

22.60

22.60

22.60

22.60

22.60

22.60

22.60

22.60

22.60

22.60

22.60

22.60

22.60

22.60

22.60

22.60

22.60

22.60

22.60

22.60

22.60

22.60

22.60

22.60

22.60

22.60

22.60

22.60

22.60

22.60

22.60

22.60

22.60

22.60

22.60

22.60

22.60

22.60

22.60

22.60

22.60

22.60

22.60

22.60

22.60

22.60

22.60

22.60

22.60

22.60

22.60

22.60

22.60

22.60

22.60

22.60

22.60

22.60

22.60

22.60

22.60

22.60

22.60

22.60

22.60

22.60

22.60

22.60

22.60

22.60

22.60

22.60

22.60

22.60

22.60

22.60

22.60

22.60

22.60

22.60

22.60

22.60

22.60

22.60

22.60

22.60

22.60

22.60

22.60

22.60

22.60

22.60

22.60

22.60

22.60

22.60

22.60

22.60

22.60

22.60

